AL-TR-1992-0061

AD-A263 875

ARMSTRONG LABORATORY

METHODS FOR CHARACTERIZING THE HUMAN HEAD FOR THE DESIGN OF HELMETS

Kathleen M. Robinette
Jennifer J. Whitestone

CREW SYSTEMS DIRECTORATE
HUMAN ENGINEERING DIVISION

APRIL 1992

FINAL REPORT FOR THE PERIOD SEPTEMBER 1990 TO APRIL 1992

AIR FORCE SYSTEMS COMMAND
WRIGHT-PATTERSON AIR FORCE BASE, OHIO 45433-6573

NOTICES

When US Government drawings, specifications, or other data are used for any purpose other than a definitely related Government procurement operation, the Government thereby incurs no responsibility nor any obligation whatsoever, and the fact that the Government may have formulated, furnished, or in any way supplied the said drawings, specifications, or other data, is not to be regarded by implication or otherwise, as in any manner licensing the holder or any other person or corporation, or conveying any rights or permission to manufacture, use, or sell any patented invention that may in any way be related thereto.

Please do not request copies of this report from the Armstrong Aerospace Medical Research Laboratory. Additional copies may be purchased from:

National Technical Information Service
5285 Port Royal Road
Springfield, Virginia 22161

Federal Government agencies and their contractors registered with the Defense Technical Information Center should direct requests for copies of this report to:

Defense Technical Information Center
Cameron Station
Alexandria, Virginia 22314

TECHNICAL REVIEW AND APPROVAL

AL-TR-1992-0061

This report has been reviewed by the Office of Public Affairs (PA) and is releasable to the National Technical Information Service (NTIS). At NTIS, it will be available to the general public, including foreign nations.

This technical report has been reviewed and is approved for publication.

FOR THE COMMANDER

Kenneth R Boff

KENNETH R. BOFF, Chief
Human Engineering Division
Armstrong Laboratory

REPORT DOCUMENTATION PAGE

Form Approved
OMB No. 0704-0188

1. AGENCY USE ONLY (Leave blank)	2. REPORT DATE	3. REPORT TYPE AND DATES COVERED
	April 1992	Final September 1990 to April 1992

4. TITLE AND SUBTITLE
Methods for Characterizing the Human Head for the Design of Helmets

5. FUNDING NUMBERS
PE 62202F
PR 7184
TA 08
WU 50

6. AUTHOR(S)
Kathleen M. Robinette
Jennifer J. Whitestone

7. PERFORMING ORGANIZATION NAME(S) AND ADDRESS(ES)
Armstrong Laboratory, Crew Systems Directorate
Human Engineering Division
HQ HSD, AFSC
Wright-Patterson Air Force Base 45433-6573

8. PERFORMING ORGANIZATION REPORT NUMBER
AL-TR-1992-0061

9. SPONSORING/MONITORING AGENCY NAME(S) AND ADDRESS(ES)

10. SPONSORING/MONITORING AGENCY REPORT NUMBER

11. SUPPLEMENTARY NOTES

12a. DISTRIBUTION/AVAILABILITY STATEMENT
Approved for public release; distribution is unlimited.

12b. DISTRIBUTION CODE

13. ABSTRACT (Maximum 200 words)

For complex helmet systems that include optical displays and enhancements, as well as advanced sound attenuation, etc., the old methods for using anthropometry in design are inadequate. In this report, approaches for characterizing the human in the design process are described that provide, for the first time, shape and contour information. These methods have begun to revolutionize the helmet design process.

14. SUBJECT TERMS
Anthropometry
Helmets
Design

15. NUMBER OF PAGES
71

16. PRICE CODE

17. SECURITY CLASSIFICATION OF REPORT	18. SECURITY CLASSIFICATION OF THIS PAGE	19. SECURITY CLASSIFICATION OF ABSTRACT	20. LIMITATION OF ABSTRACT
Unclassified	Unclassified	Unclassified	UL

NSN 7540-01-280-5500

Standard Form 298 (Rev 2-89)
Prescribed by ANSI Std Z39-18
298-102

PREFACE

This research was carried out with financial support from the Helmet Mounted Systems Technology program office, and contractual support under contract number F33615-89-C-0572. The authors would like to thank several people who contributed their efforts. Thanks go to Mary Gross of Beecher Research Inc. who edited the three-dimensional data files and wrote the program to select the 16 candidate subjects, to Dennis Burnsides of Cytronics Corp., and Thomas Churchill and Phillip Walker of Anthropology Research who extracted and plotted the slices for the scale drawings. Thanks also go to Robert Beecher, of Beecher Research Inc. who prepared the selected heads for the milling process.

SUMMARY

Although computer-aided design (CAD) software packages have been employed by engineers to develop designs for improved protective equipment, the three-dimensional human characterizations consisted of three-dimensional data derived from two-dimensional measurements or sparsely located three-dimensional "landmarks," a process that lacks accuracy and consistency. With the advent of more complex helmet systems that now include night vision goggles and helmet mounted displays, as well as advanced sound attenuation components, the imprecision and inadequacy of the old style of anthropometry becomes painfully apparent. For such systems information on the shape, or change in the surface curvature, is now a necessity. In fact, use of the old style of anthropometry can create problems rather than resolve them.

In this report, two approaches for characterizing the human in the design process are described that provide, for the first time, shape and surface contour information tied to traditional anthropometry as well as information regarding the manner in which the human head "wears" a protective helmet or other equipment designed for human interface. These methods have begun to revolutionize the design process and have provided insight into the inaptitude of some of the more traditional practices.

TABLE OF CONTENTS

LIST OF FIGURES

LIST OF TABLES

CHAPTER ONE
INTRODUCTION

With the advent of more complex helmet systems that now include night vision goggles and helmet mounted displays, as well as advanced sound attenuation components, the old style of anthropometry (human body measurements taken with calipers, tape measures with head boards etc.) is no longer adequate. For such systems, data on the shape, or change in the surface curvature, is now a necessity. In fact, use of the old style of anthropometry can create problems rather than resolve them.

The source of the problem is one of alignment (how things line up in space) with respect to the item being designed. This has been identified by numerous researchers in a variety of fields and has been called "observer-inherence." In simple terms, this means that the positioning and orientation of the reference axis system can affect the results more than the size and shape do. Research on fit of helmets with optical systems has indicated that the reference axis system is particularly critical for such systems, although this same problem occurs with other types of equipment as well.

Many old style measures are distances taken with respect to a standard reference "plane," usually the international standard Frankfurt Plane. In ASCC AIR STANDARD 61/83, this plane is described as "...a standard plane for orientation of the head. It is established by a line passing through the right Tragion (the notch located just above the cartilaginous flap of the flesh in front of the ear) and the lowest point of the right eye socket." It was thought that this alignment system would result in consistent measurements from subject to subject. However, as is demonstrated below, it can be shown that the measurements which result with the use of this alignment plane, or any other purely anatomical landmark based alignment system, provide inappropriate measurements for helmet design.

Figure 1 was prepared to illustrate the problem. It consists of contour plots of two male flyers who have nearly identical head lengths and breadths. The only difference in the two plots in parts a and b is the way the subjects are aligned. Part a shows the contours aligned according to the Frankfurt Plane with the origin at the tragion. Part b shows the same subjects aligned as they actually wore the HGU 55/P helmet.

As can be seen, the helmet alignment radically changes the reference planes and with it most of their measurements. The direction "up" in the Frankfurt Plane was along the X axis shown. In the helmet, this axis no longer points "up" for both subjects. This means that the "back of the head" and the "top of the head," which are commonly used reference "points" in traditional measurement systems, have moved as well. In addition, note that the pupils (P1 and P2) appear to be almost co-located in part a, but they appear to be nearly half an inch apart in part b. Clearly, pupil, ear etc. positioning in actual helmets are very different

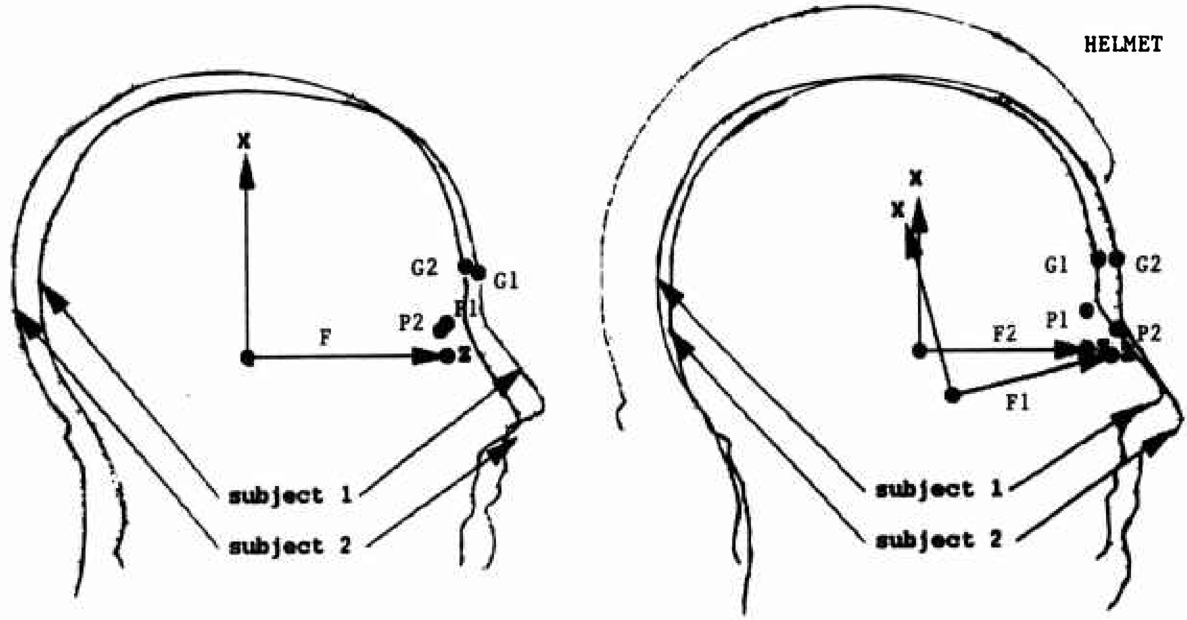

a) Traditional Measurement Alignment

F=FRANKFORT PLANE BOTH SUBJECTS
G1=GLABELLA FOR SUBJECT 1
G2=GLABELLA FOR SUBJECT 2
P1=PUPIL FOR SUBJECT 1
P2=PUPIL FOR SUBJECT 2

b) Helmet Alignment

F1=FRANKFORT PLANE FOR SUBJECT 1
F2=FRANKFORT PLANE FOR SUBJECT 2

Figure 1. Traditional alignment versus actual helmet alignment.

from the positions that traditional anthropometry suggests.

If the subjects are not aligned as they would wear the helmet before measures are taken, then many of the most critical measures, such as pupil-to-top-of-head, or pupil-to-back-of-head, provide misleading information. Top-of-head (also called vertex) and back-of-head are dependent upon how top and back are defined, i.e. the axis system. Analysis of the fit and anthropometry of several helmet systems revealed that in many cases the measures can be different by inches strictly due to the orientation used. Since traditional anthropometry does not capture the head and face surface, it is not possible to realign the heads once the subjects are gone. This limitation makes many of the traditional measurements not only inappropriate but essentially useless.

Cheverud et. al. (1983) attempted to resolve the problem of axis system dependency or observer-inherence using distances between a small number of specific points and finite element analysis. With this approach, shape is considered to be the relative distances, areas, or volumes between the points and does not represent change in curvature. Lele and Richtsmeier (1991) used the same sort of variables for defining shape and Euclidian distance matrix analysis for the same purpose. These methods may in fact resolve the problem sufficiently for the purpose of comparing biological shapes or the classification of species, their intended purpose. However, on the human head there are not many landmarks which are palpable in the cranial region, (where helmets rest), which limits their applicability. Probably most important though, is the fact that, for helmet design it is not so important to have axis system independence as it is to have axis systems which are helmet or design dependent.

In order to arrive at helmet based axis systems, it must be possible to align people according to "helmet criteria." With the old style of data, such as point to point distances, circumferences and arcs, and three-dimensional coordinates on only a few points, usually 30 to 40 on the human head, no data on the contours is provided. This makes it impossible to derive much of the critical helmet based criteria, because the curvature of the head is crucial to how the helmet fits. Figure 2 illustrates this limitation. In this Figure, the 3D coordinates of 22 traditional landmarks are shown, (the L marks), along with a subject's contours in part a and without the contours in part b. These are landmarks that fall on or near the mid-sagittal plan, or on the subject's right side. Adding the left side landmarks would increase the number of landmarks to 32. This is a large number of landmarks for a traditional data set. As can be seen, once the contours are removed little information remains. This is complicated further by the fact that there are few landmarks which are readily and consistently palpable on the top, back and sides of the head. Nearly all traditional landmarks on living people fall on the face. Clearly the landmark data is insufficient to align the shape of the head to that of the helmet. Therefore, to answer the needs of modern helmet systems, a new type of data which captures both the contours and the key points is needed.

In this paper, new research to address this need is presented. Contour data on the head and face of Air Force aviators has recently become available, and it is now possible to incorporate it into the design of helmet systems. This should enable the developers to produce superior systems at a much cheaper cost. Better definition of shape should reduce the amount of error and refitting needed, should enable designers to fit more closely to the head which will reduce surface area and weight, and should enable them to design the systems to fit more people with the fewest number of sizes.

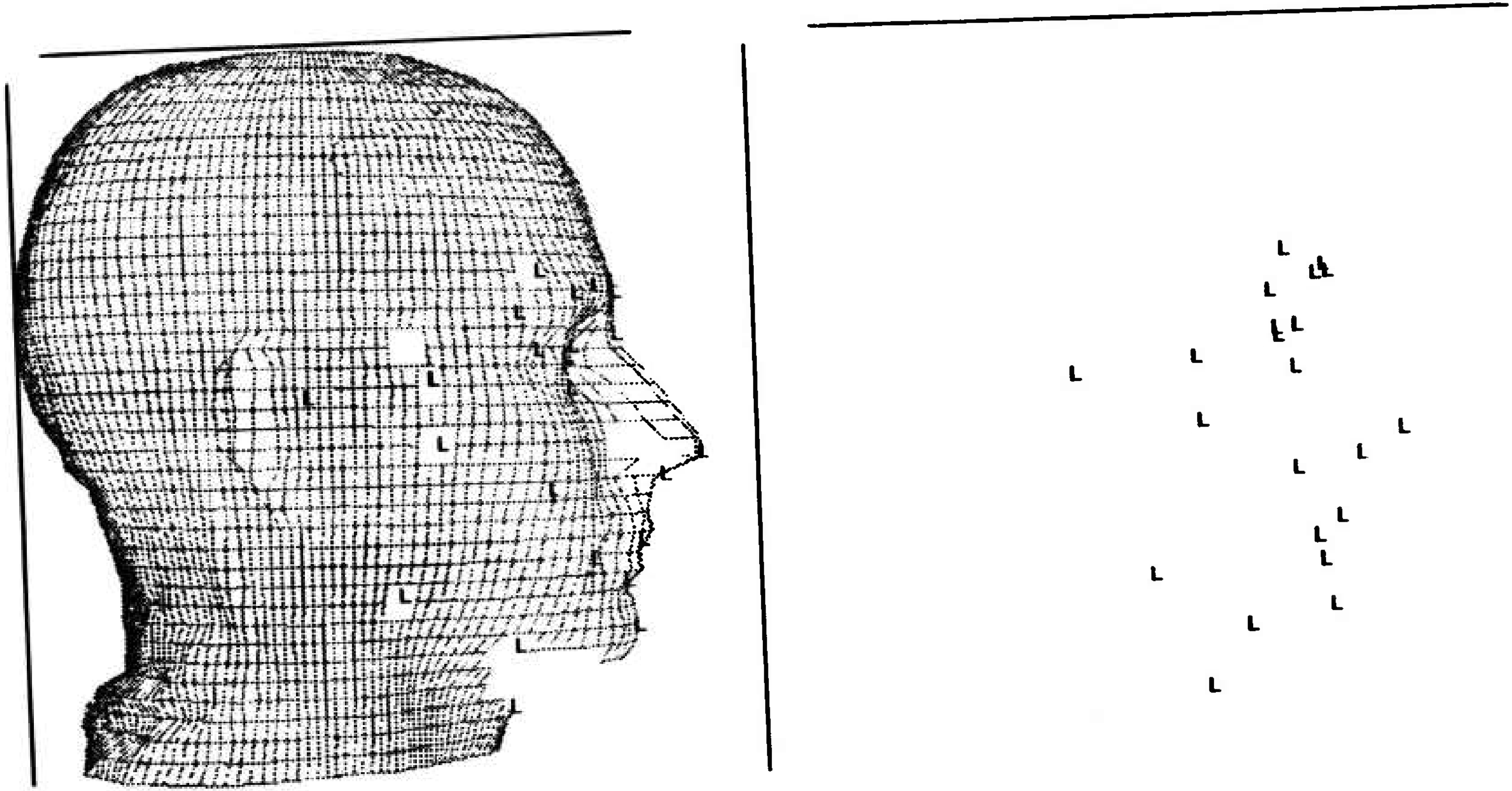

a) With contour data

b) Without contour data

Figure 2. Traditional 3D landmarks with (a) and without (b) contour data

CHAPTER TWO
METHODS

Two different approaches for characterizing the human head for helmet design are described here. One for population definition when the equipment is unknown or unavailable, and one for population definition with respect to a particular item of equipment. The first approach is one which might be taken to provide information for a requirements document or as a design aid before an item exists. It leaves the integration of the helmet with the forms up to the designer or investigator.

The second approach requires the use of an existing helmet and provides the designer with spatial locations of key human features, (such as the pupil), with respect to that helmet. The approach also allows the designer to visualize how much room there is between helmet components and the human. This is useful if new earcups or visual devices, etc. are to be added to existing helmets, or for adding components such as air bladders for positive pressure breathing systems, etc.

Data from a single data survey was used to illustrate these approaches. This survey is described briefly below followed by a description of each approach.

THE DATA SET

The data used for this effort were taken from a recent survey of Air Force aircrew members. Of the 353 subjects of whom data were collected, 326 were male rated officers, and were used for developing these methods. The data were collected over several months in 1990 at sites throughout the continental U.S. The data collection methods and results are documented in greater detail in a report by Blackwell et.al. 1992, but are briefly described here.

Essentially, the data for an individual subject consists of three types; three-dimensional high resolution surface scans, a set of 32 three-dimensional landmarks (special reference points such as the pupil, the tip of the nose, etc.), and a set of traditional anthropometric measures. The subjects were scanned with and without their flight helmets and masks (when available) with a Cyberware Echo Digitizer. The Digitizer, which captures the surface data in about 12 seconds as it circles around the subject's head, provides cylindrical data in the form of radius values from the center of rotation. As 256 points are digitized along each vertical line projected down the surface at regular intervals, the resulting data set consists of an array of 512 x 256 radii (approximately 130,000 surface points). The resolution then, is approximately 1 mm. For the scans without equipment, tight fitting, specially prepared rubber caps were used to compress the hair, and several landmarks were pre-marked with 2mm diameter dots for easy identification. An additional unencumbered scan was collected for each subject with their head in a "chin-up" position to augment the first data set.

The digital surface data shown in Figure 3 is of an unencumbered head scan. A helmeted scan is shown in Figure 4. A list and description of the 32 landmarks identified are provided in Appendix A. Given the nature of the surface scan data, additional landmarks could be extracted if desired. A list and description of the traditional anthropometric measures of the head and face collected on this sample are included in Appendix B.

CHARACTERIZATION WITHOUT A HELMET

This approach has three basic steps: the digitization of the head and face surfaces of a sample of subjects from the population of interest, the statistical selection of a small number of representative cases from these, and the creation of three-dimensional forms of these candidates. The forms are reproductions of the representatives as half-scale plots of the contours, as digital data sets, and as physical forms such as plaster or plastic.

Selection of Cases

The goal of this selection was to reduce the number of subjects to a manageable number while retaining sufficient variability. At present, there are no simple shape or contour measures available for use in this statistical selection. An attempt was made to reduce the traditional type variable sets to a smaller number using principal component analysis. Despite trying different component rotations, using distance measures extracted from the scans, angular measurements, different axis systems with these distance measures and angles ,etc. the best that could be accomplished indicated that 15 factors still left 20% of the variance unexplained. This variable reduction technique was deemed unsuccessful. It is possible that the inability to reduce the number of variables with this method was due primarily to the use of a landmark-based axis system.

Given the failure of the principal component variable reduction attempts, it was decided to instead select a stratified sample of subjects from the data set using a few variables which intuitively seem to be important to helmets. Two measures which have traditionally been used in helmet sizing (Zeigen 1960, Simpson 1974) are head length and head breadth. Measurement descriptions for these measures are included in Appendix B. These measures also seem to be more linked to shape, or at least the measurer's perception of shape and head symmetry, than measures that are linked to the Frankfurt Plane, such as pupil-to-top-of-head.

Shown in Figure 5 is a bivariate plot of head length versus head breadth for this sample. Target head length and head breadth points were selected to spread out across the distribution for these two variables. These points are also shown in Figure 5 as well as listed in Table 1 below. Subjects to

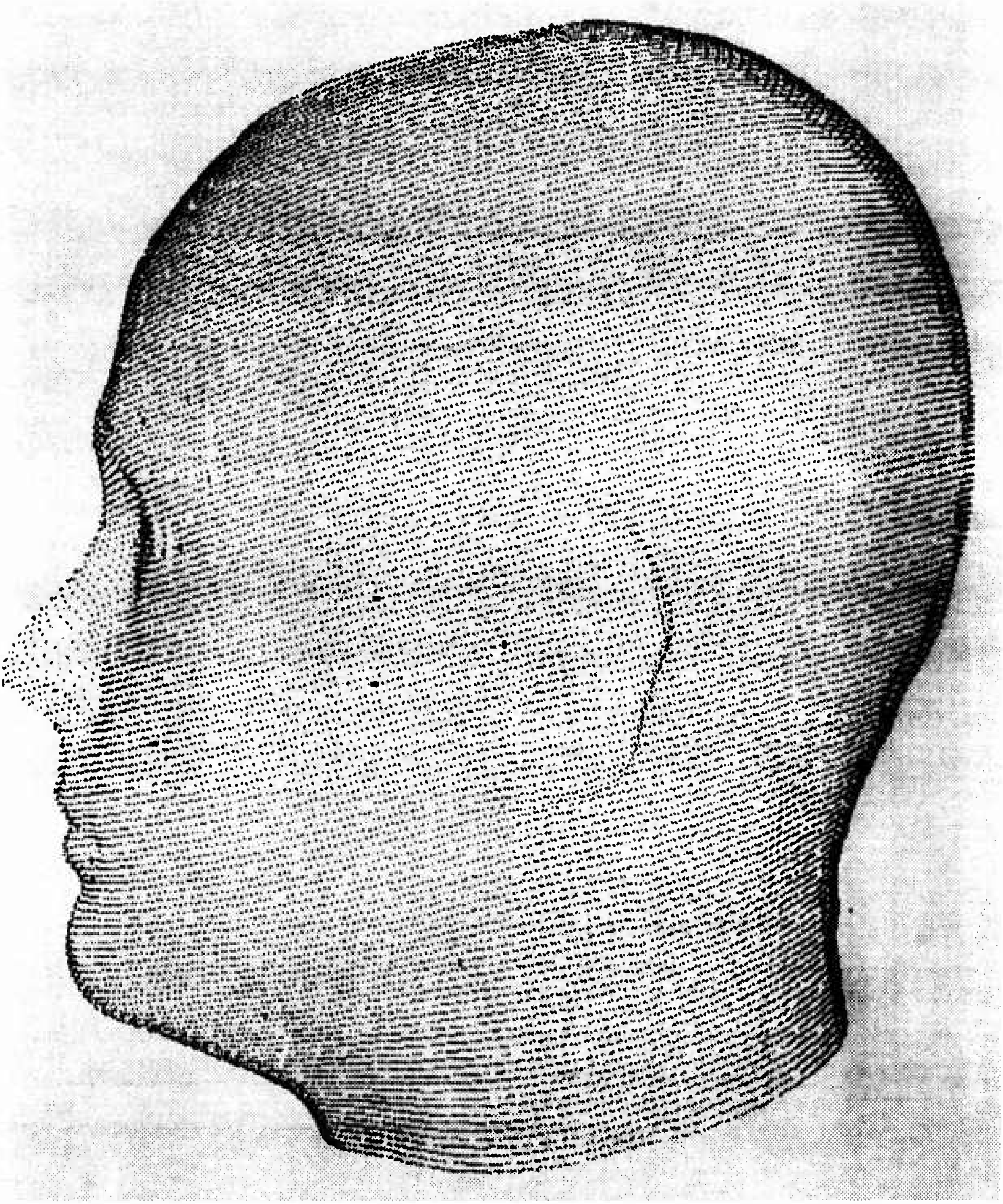

Figure 3. Plot of one unencumbered subject.

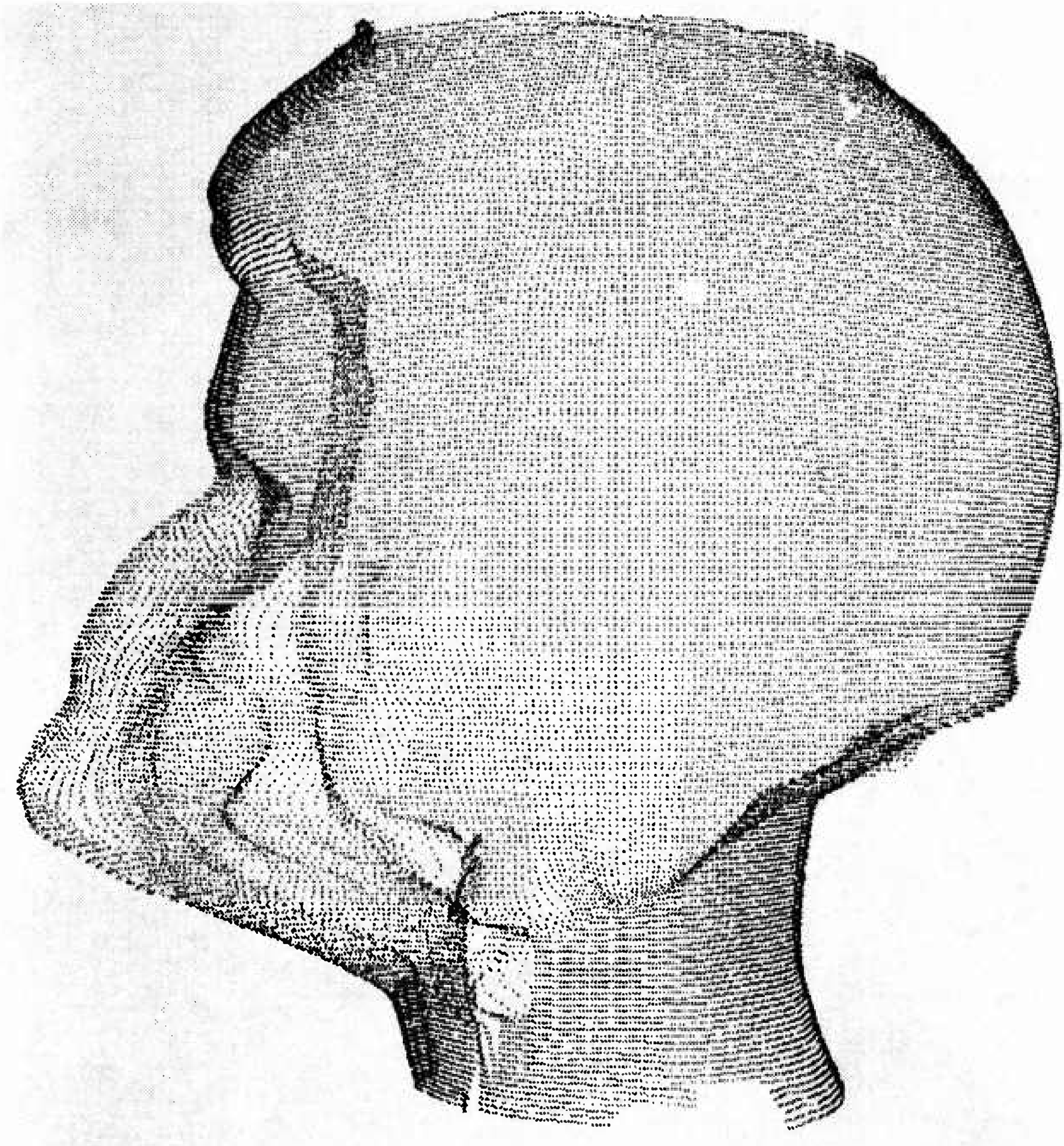

Figure 4. Plot of one encumbered subject.

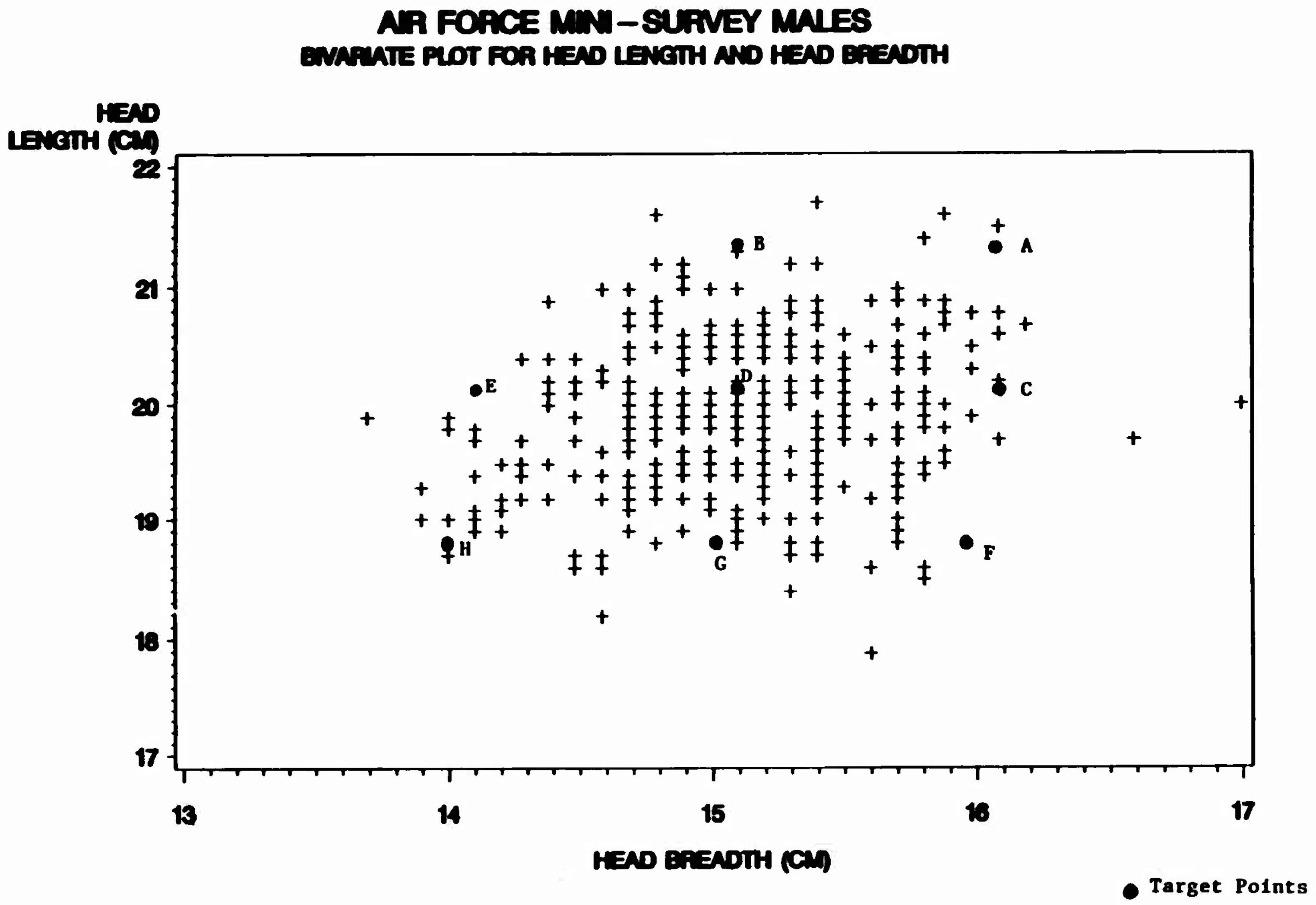

Figure 5. Head measures from the 1990 head survey and target points for the reduced set of subjects

represent the population who fell within + or - 4 mm of the target points were then selected. Two subjects were selected for each point in an effort to obtain some variability separate from the target variables, such as some shape variability, pupil location variability etc. The subject numbers, head length, and head breadth sizes for each of the subjects are listed in Table 2. It would be desirable to select more subjects and study the variability in these regions, and possibly to derive composite regional forms instead of using the original subjects. This is planned for future work. At present the difficulty in selection, preparation and use of the data made the use of additional representatives too costly.

TABLE 1
TARGET POINTS

Point	Head Length(cm)	Head Breadth(cm)
A	21.4	16.1
B	21.4	15.1
C	20.1	16.1
D	20.1	15.1
E	20.1	14.1
F	18.8	16.0
G	18.8	15.0
H	18.8	14.0

TABLE 2
SUBJECTS SELECTED FOR EACH TARGET POINT

Point	Subject	Head Length (cm)	Head Breadth (cm)
A	350	21.5	16.1
	328	21.6	15.9
B	319	21.3	15.1
	281	21.2	14.9
C	81	20.2	16.1
	36	19.9	16.0
D	188	20.1	15.1
	290	20.1	15.1
E	300	20.2	14.4
	329	20.1	14.4
F	229	18.9	15.7
	161	18.8	15.7
G	246	18.8	15.1
	317	18.9	14.9
H	52	18.7	14.0
	243	18.9	14.1

Preparation of Forms and Drawings

After the selection of the representative candidates, the next challenge was to provide the information in a form that designers could use. The simplest output is the raw data files in ASCII format on magnetic tape. These files represent the data in terms of longitude, latitude, and radius values, Cartesian coordinates or both. However, the raw data sets are too large for most commonly available visualization or computer-aided-design software. Therefore, two immediate output forms that could be more commonly used were devised. The first was to take perpendicular slices through each representative case and present the slices as scale drawings that users could reconstruct as at least crude 3D forms. The intention was to provide scale drawings as part of requirements documents to assist designers. A second was to reproduce the data as a head form.

For the scale plots, three orthogonal contours were extracted and plotted at 1/2 scale. A fourth slice was added which is parallel to one of the first three and perpendicular to the others for further shape definition. Illustrations of the slices are shown in Figures 6 and 7. The final plots for all of the 16 subjects are provided in Appendix C.

The first slice selected was one intended to represent the mid-sagittal plane. This is the plane which divides the head into right and left halves. The slice was selected by first finding the glabella landmark and the vertical contour closest to this point on the anterior portion of the head. Next, the posterior contour was located which was closest to 180 degrees from the anterior one. The axis of rotation is the perceived head center (rather than only the scanning system's center of rotation). This slice was then visually checked with respect to all of the surface data from that individual to verify that there was a minimal amount of lateral deviation of the head.

For the next slice, a plane was desired to represent the coronal plane that passes close to where the head breadth measure is taken. To define this slice, the tragion landmarks were used. Experience has indicated that the maximum head breadth occurs somewhat posterior to the ears, so this slice was selected at 3mm posterior to the tragion landmarks. This slice was perpendicular to the first slice at the level of the right and left tragion.

The third slice selected was a transverse plane, perpendicular to the first two planes and passing through the right pupil. The fourth was parallel to this slice but passing through glabella.

A sample of the output (reduced further and not to scale) is illustrated in Figure 8. In this Figure, all four views are shown. The first is the sagittal plane slice called the right side view (mid-sagittal plane) which appears at the upper left of

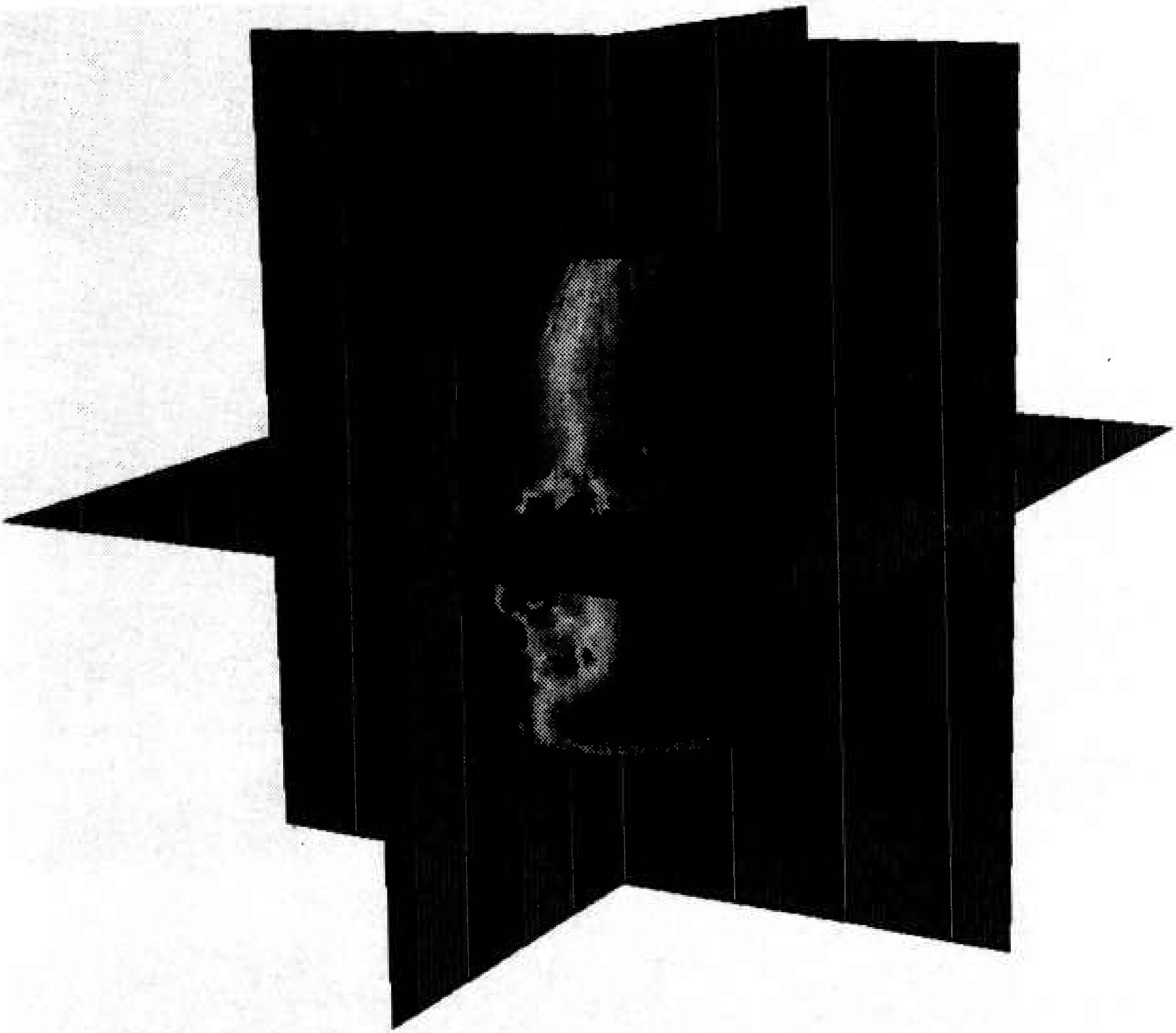

Figure 6. Illustration of slices extracted with tranverse pupil slice.

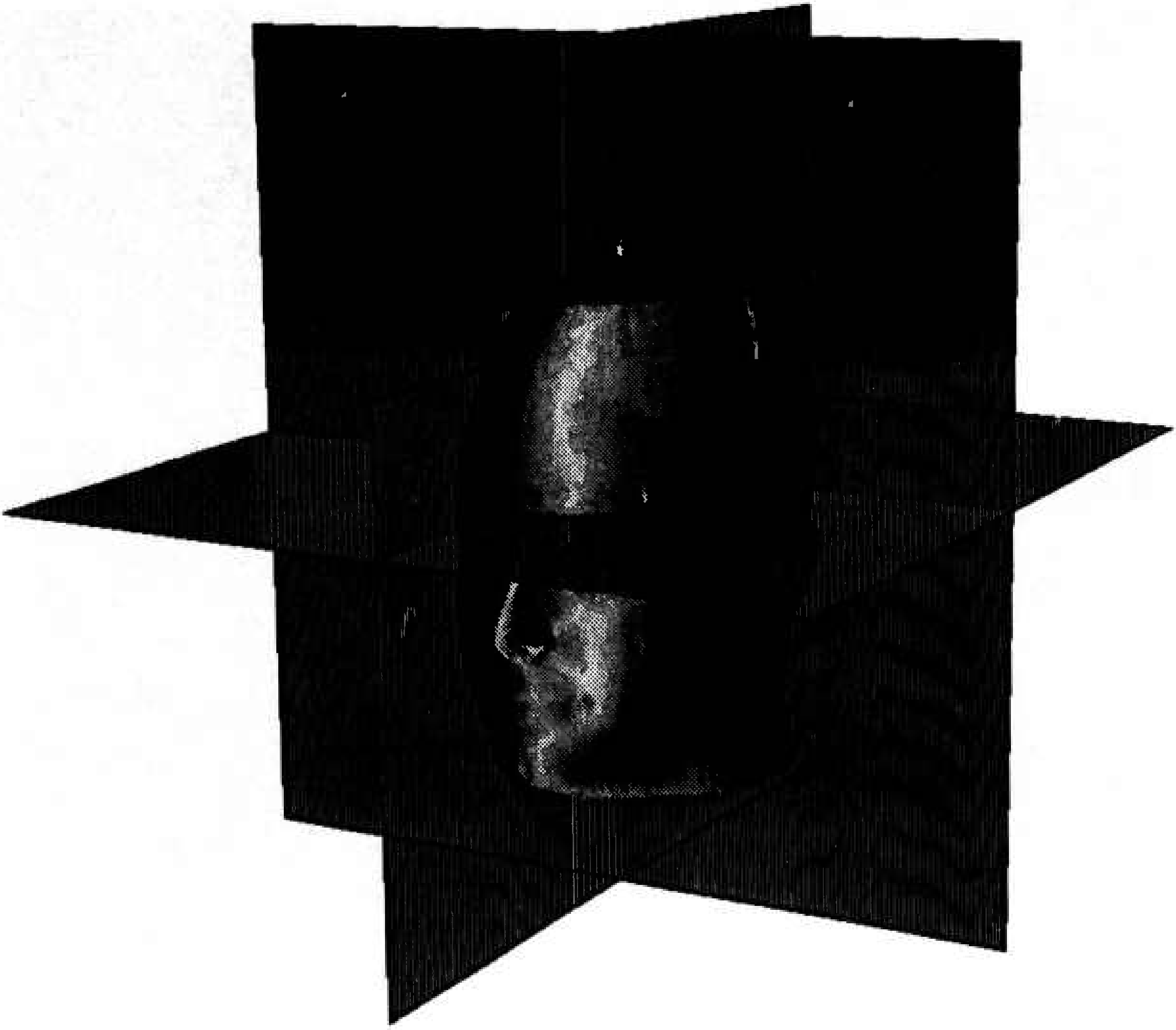

Figure 7. Illustration of slices with tranverse glabella slice.

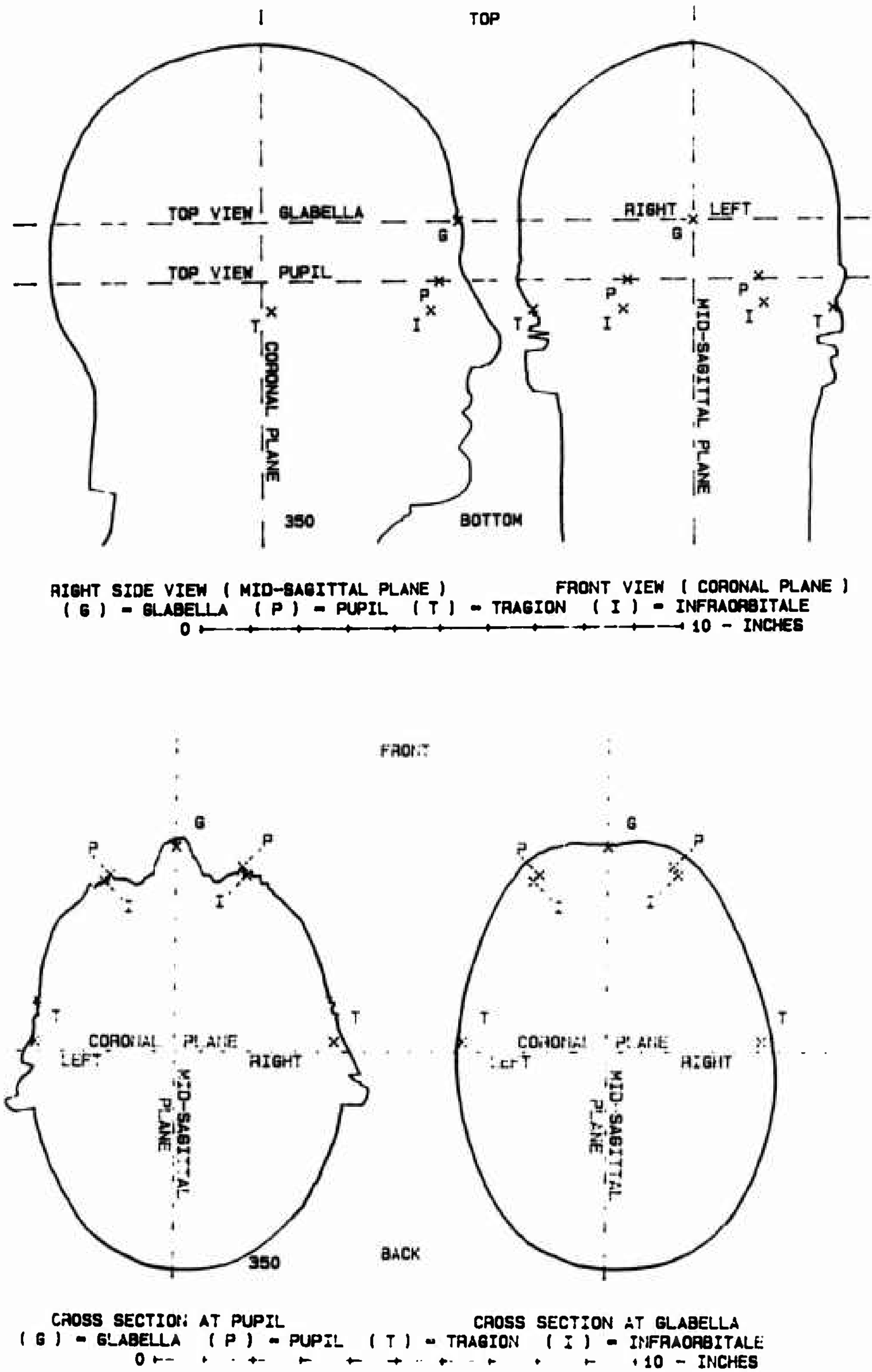

Figure 8. Sample of slices from one case.

this figure. The dashed lines illustrate where the other slices occur. For example, the dashed line which is vertically placed on this view shows the placement of the coronal plane slice called the "front view (coronal plane)." A few reference landmarks are also illustrated. The coronal plane slice itself appears in the upper right corner of the Figure. The other two views are the transverse slices at glabella and pupil. These can be thought of as views of the head looking down from the top.

The selection of slices was very much axis system based so it will be important for the users of this information to realign the plots to reflect assumptions about the placement of the helmet on these heads. (The slices taken from the scan data were based on Frankfurt Plane alignment.) Figure 9 illustrates two such alignment concepts. The first one, part a, might be used if the helmet is to have a form fitting liner and only a width adjustment for the optics. In this case, the subjects are aligned at their pupils and along their forehead curvature but the back of the head is not aligned. The second alignment, part b, might be used for a helmet with a form fitting liner and some fore-aft and vertical adjustability in the optics. In this case, the cranial portion is aligned using a contour fitting method. This aligns the top and back portions of the head better which may provide more stability in a design, as well as a smaller helmet "profile" with the same quality of fit.

Due to the use of the Frankfurt Plane alignment for slice extraction, a re-alignment of the sagittal views, as in Figure 9, will cause a "misalignment" in the other slices. In other words, the transverse cross sections at pupil and glabella and the coronal cross section will be rotated and translated to positions on one person which are different from the positions on another. A better way to use this cross section method would be to place the subjects in the assumed helmet alignment prior to extracting slices and extracting the slices in "helmet" defined planes. In this way, the slices would be taken in "helmet" comparable spots for all the subjects. As more becomes known about how helmets are located in 3D space with respect to the head, perhaps some generic helmet alignment criteria can be devised to replace the Frankfurt alignment.

For the physical forms, the raw data were first modified to remove the nose, chin and ears. The subject selection scheme did not account for variability in these regions, and it was felt that if they were included on the forms designers might assume that they represent the population and use them to design masks, ear cups, etc. Furthermore, with these features removed it would be easier to later add in components which do reflect the variability in these regions in a manner which is appropriate to the particular design needs. For example, ear envelopes which describe the entire region in which an ear is likely to appear might later be added to the individual heads.

The head form data were then put into a standard format for

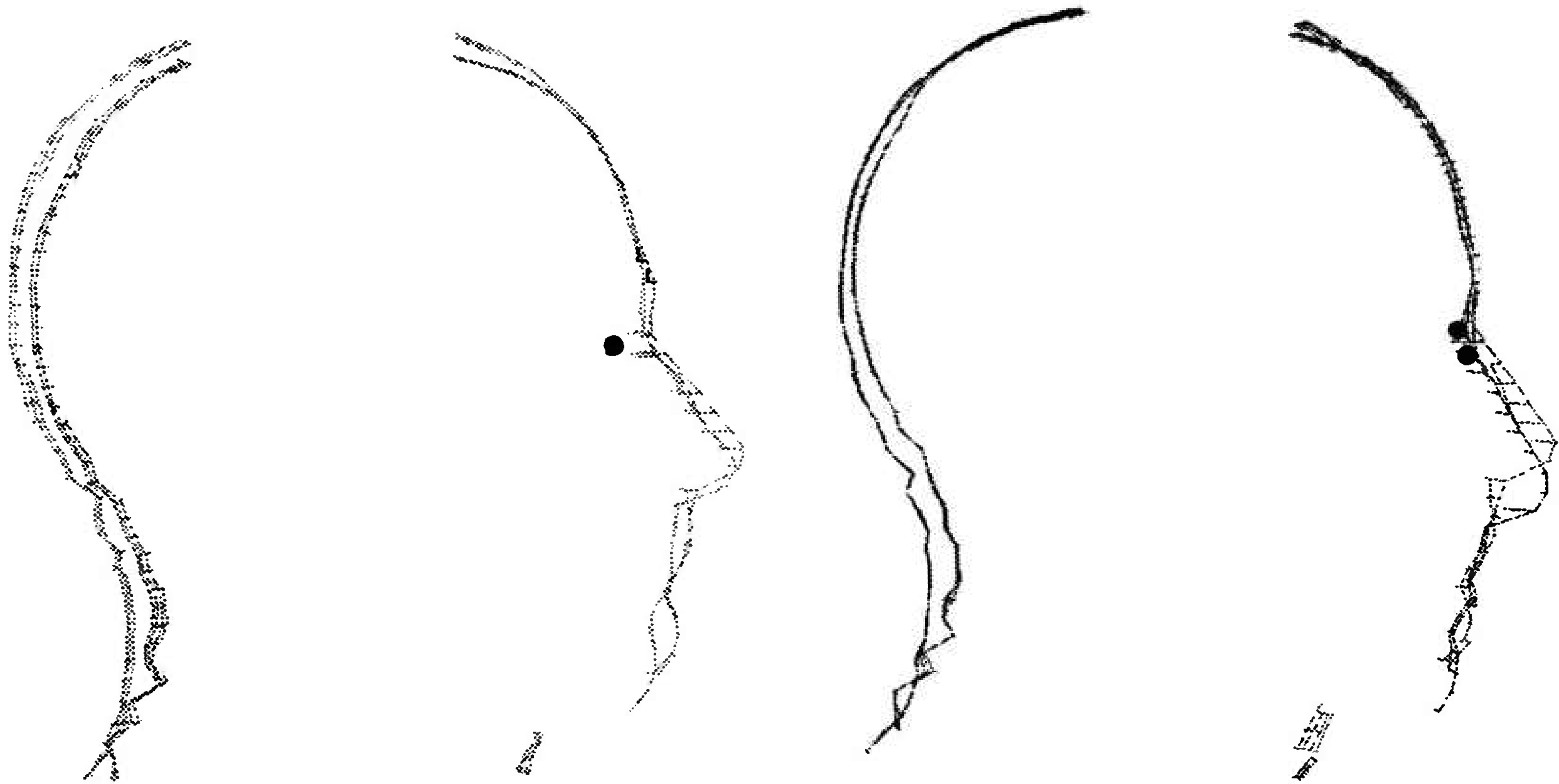

a) pupil and forehead alignment

b) cranial region alignment

Figure 9. Two alignment concepts

milling and were carved out using a numerically controlled milling machine. An illustration of one of the forms is shown in Figure 10.

CHARACTERIZATION WITH HELMET

When there is data available regarding the helmeted subject, some additional steps can be taken to determine where to place attachments or additional equipment or even the areas or volumes left for placement of liners. The helmeted scans, when linked with the scans without helmets, provide the investigator with the ability to determine where key features, such as ear or eye points, fall with respect to the helmet. Plots showing the two scans merged appear in Figure 11. As can be seen, the registrations of the two scans allows the investigator to "see" where the person is inside the helmet and mask.

Theoretically, the helmet neither changes in shape nor size, so landmarks on it can be viewed as constants, unlike the behavior of landmarks on people. Therefore, once the individual subject scans are linked to a given helmet, a helmet-based axis system can identify the variability of people within the helmet. In other words, the helmet axis system can be used to standardize the alignment and define the population variability. Illustrations of a true helmet-based alignment are shown in Figures 12-16. Figures 12 and 13 show two people wearing the same HGU 55/P helmet in side and top views respectively. Figures 14 and 15 show these same subjects and alignments but unencumbered.

The large amount of data makes these plots difficult to see and this problem gets worse as more subjects are added. To assist in the visualization of the data from multiple subjects, the data were reduced to show just one or two contours at comparable places on each subject (with respect to the helmet). Figure 16 shows plots of eight subjects within the HGU 55/P size medium helmet in side and top views. Note that in the side view, (part a), the subjects seem to fall close together, but in the top view, (part b), there is one subject that sticks out at the left by comparison with the others. This could result if the subject had to wear the helmet askew in order to obtain accommodation in the fore-aft direction. This asymmetry may have been tolerable in this helmet since it did not have an optical system. However, such asymmetry was noted as a problem for optics focusing in bi-ocular helmet systems in recent testing (Blackwell et. al. 1992). Several subjects could not get the optics focused in both eyes at the same time. No asymmetry could be detected for these subjects using traditional measures. However, the asymmetry could be attributed to the manner in which the subject fit inside the helmet.

An example illustrating the use of this method was undertaken to estimate ear locations within the size medium HGU 55/P helmet. First, each unencumbered scan was linked to the scan with the helmet by first using landmarks found on the face that were common to both scans and then "fine tuning" the alignment by

Figure 10. Illustration of one of the 16 headforms.

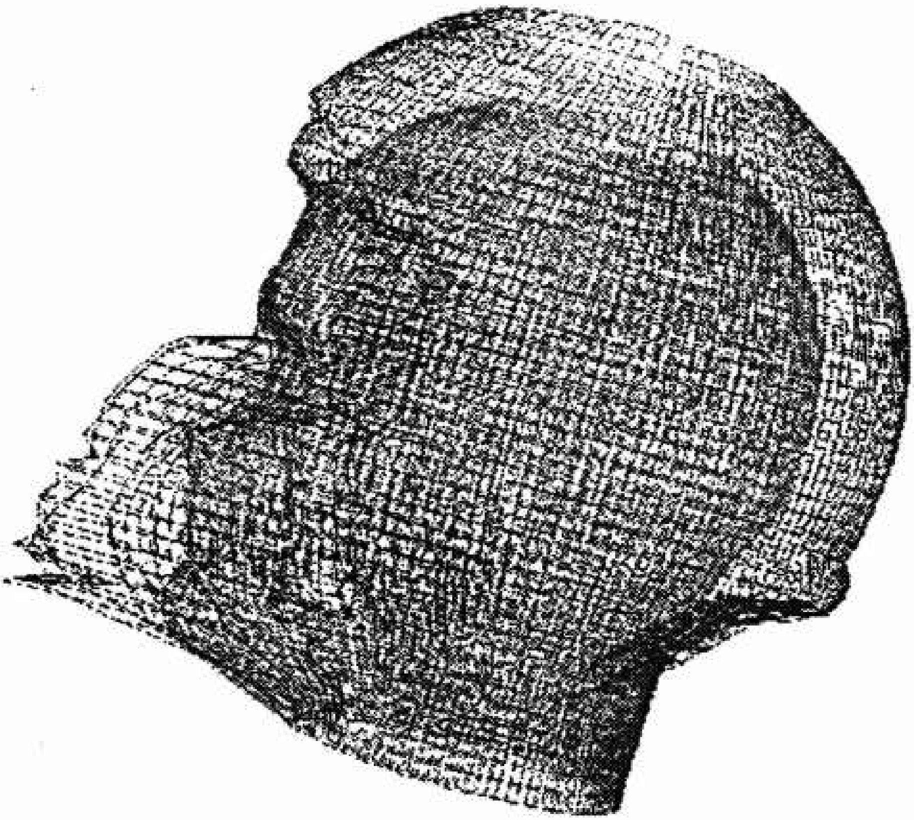

a) Side view

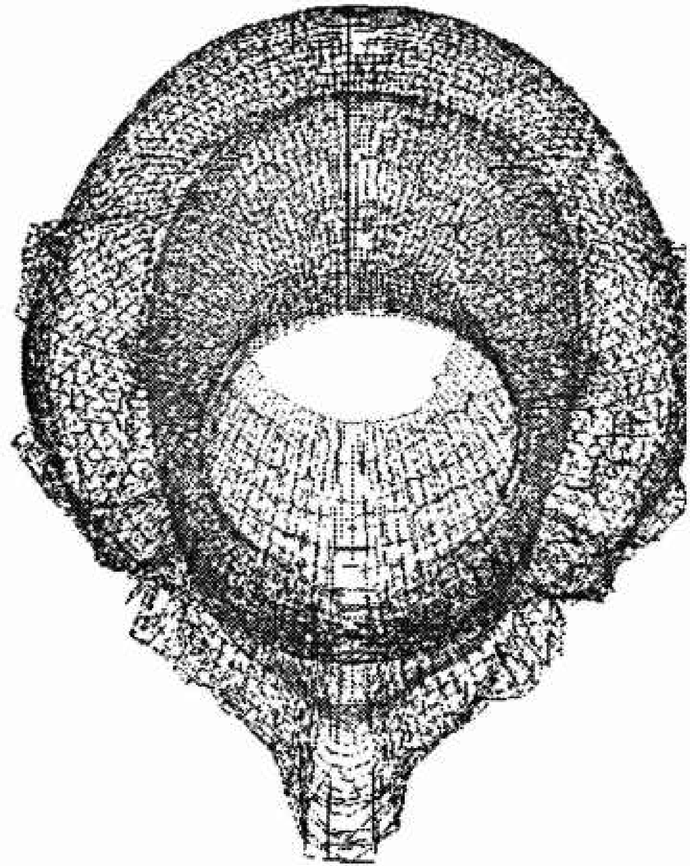

b) Top view

Figure 11. Merged plot of encumbered and unencumbered scans.

Figure 12. Two subjects in the HGU 55/P size medium helmet alignment,encumbered side view.

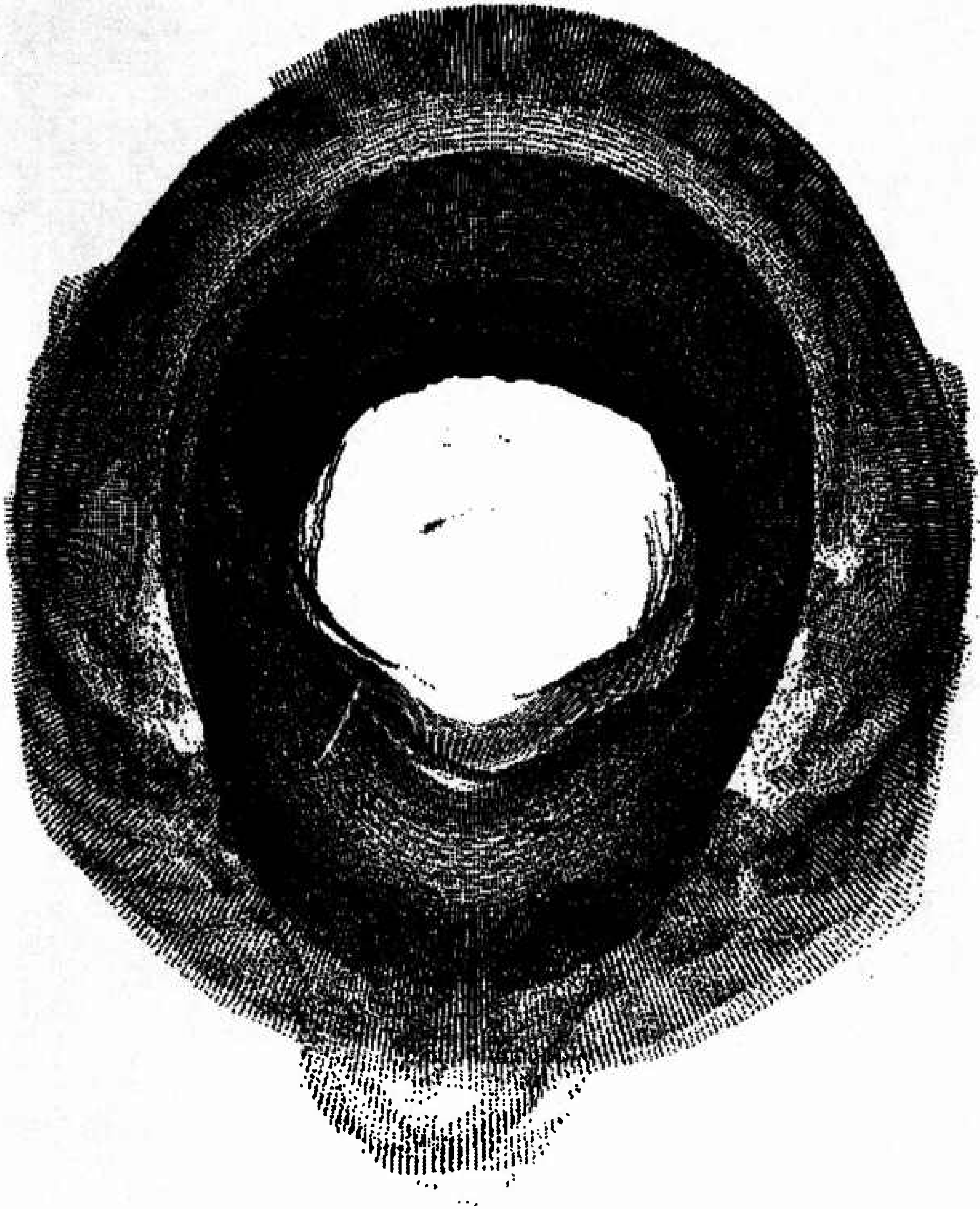

Figure 13. Two subjects in the HGU 55/P size medium helmet alignment, encumbered top view.

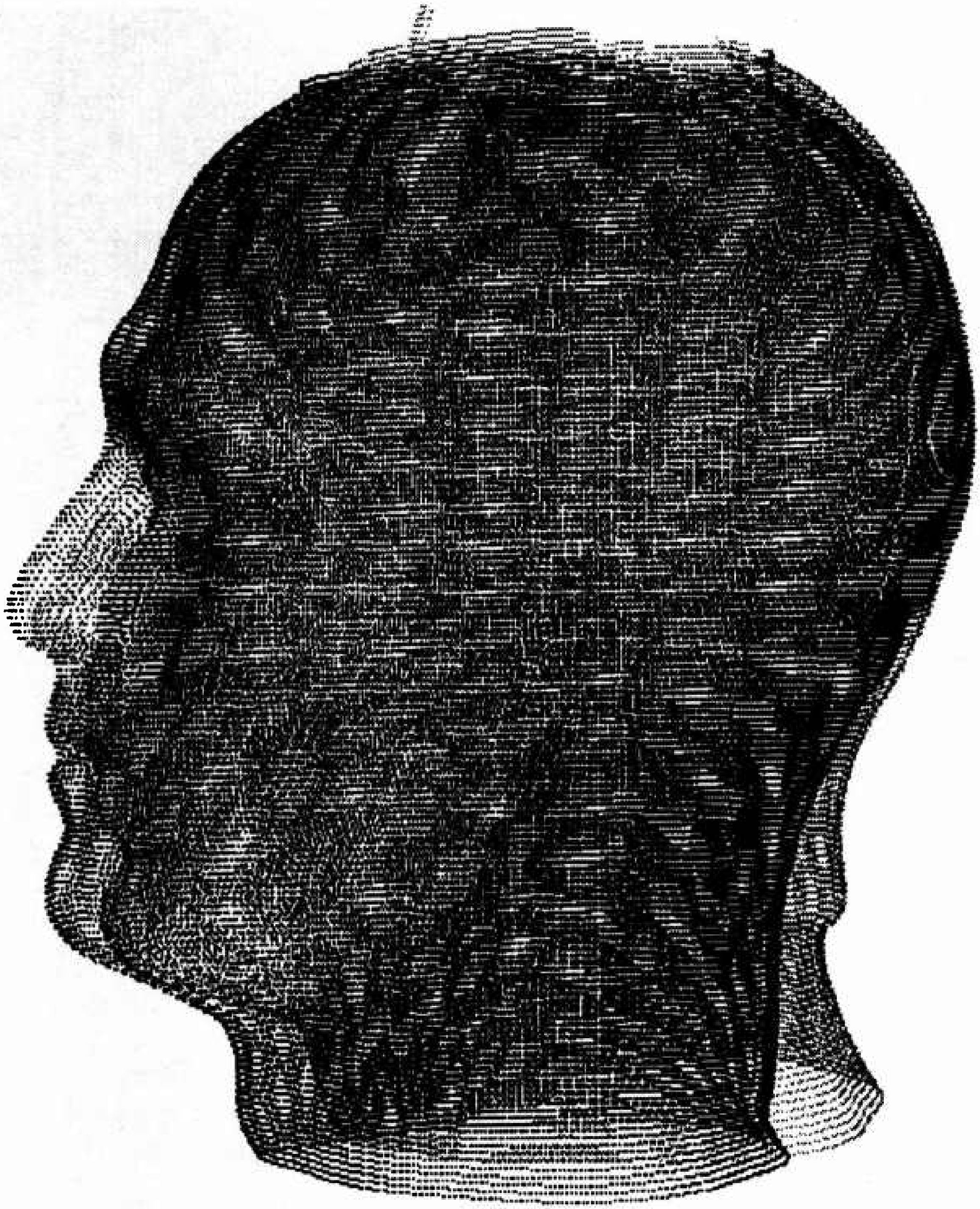

Figure 14. Two subjects in the HGU 55/P size medium helmet alignment, unencumbered, side view.

Figure 15. Two subjects in the HGU 55/P size medium helmet alignment, unencumbered top view.

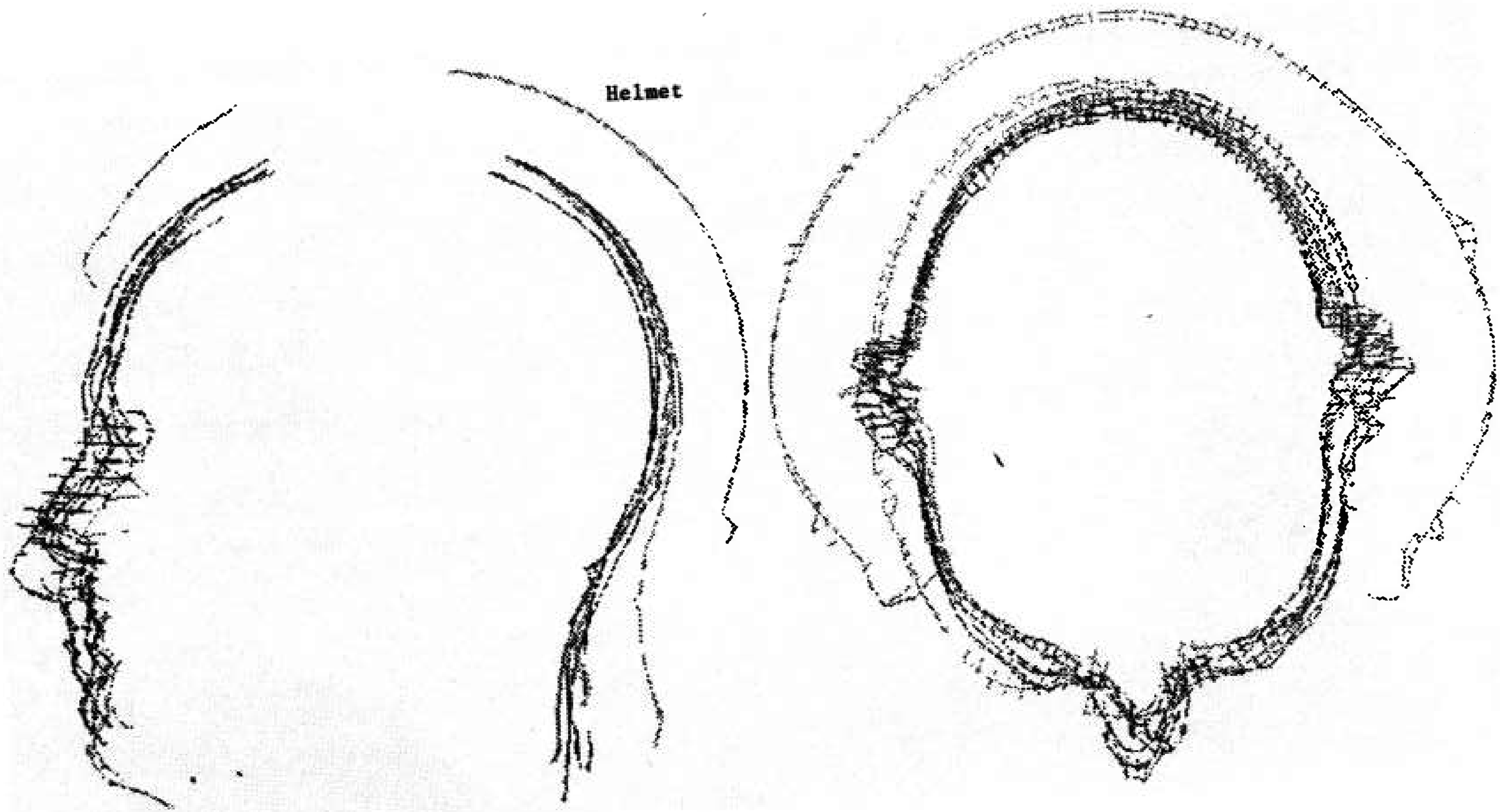

Figure 16. Eight suhjects in the HGU 55/P size medium helmet alignment, reduced data plots.

registration of the common visible surfaces. Symmetric landmarks which could be consistently located were selected from the helmets to define the helmet axis system. The scans without the helmet were transformed to this helmet axis system for each subject. The data from all subjects were linked according to the now common helmet axis system. (Note this was done only for a few subjects who wore the size medium helmet.) Finally, the locations of ear points including tragion, top-of-ear, back-of-ear, and bottom of ear, for all of the subjects, were plotted with respect to the helmet contour. An illustration of an ear point plot is shown in Figure 17. A similar plot could be created for the pupils or any other landmark.

The full ear for all of the subjects could also be overlaid in three-dimensional space to form an ear region within a helmet. Additionally, the full human surface design envelopes could be three-dimensionally mapped for the population with respect to the internal surface of the helmet shell. A "surfaced" scan within a helmet is shown in Figure 18 which illustrates the detail available on the ear. Much visualization information is lost in flat gray scale plots for paper reports. Color and 3D visualization available on graphics workstations greatly enhance the use of this information.

DISCUSSION

The two design approaches described here provide, for the first time, shape and surface contour information tied to traditional anthropometry and population information regarding the manner in which the human head "wears" a protective helmet or other equipment designed for human interface. These methods have begun to revolutionize the design process and have provided insight into the inaptitude of some of the more traditional practices. For instance, the development of these methods has demonstrated that the commonly used Frankfurt Plane, developed to standardize traditional anthropometry, is not suited to studying shape variability within a population for equipment engineering purposes. Further, the ability to "visualize" anthropometry by viewing the entire surface topology has permitted a better understanding of human variability.

However, these methods have their limitations as well. The main drawback of the contour plots is that the plots only line up in space for the alignment system used to extract the plots. For this method to be most effective, it would be best if the alignment system is established before the cross-sections are selected. Selecting an appropriate alignment system is guesswork at this time since no tested "generic" helmet alignment system exists. Research into the manner in which helmets align to heads is ongoing. As the data bases of encumbered and unencumbered topology are correlated with quality of fit information, it should be possible to effectively develop "generic" alignment schemes.

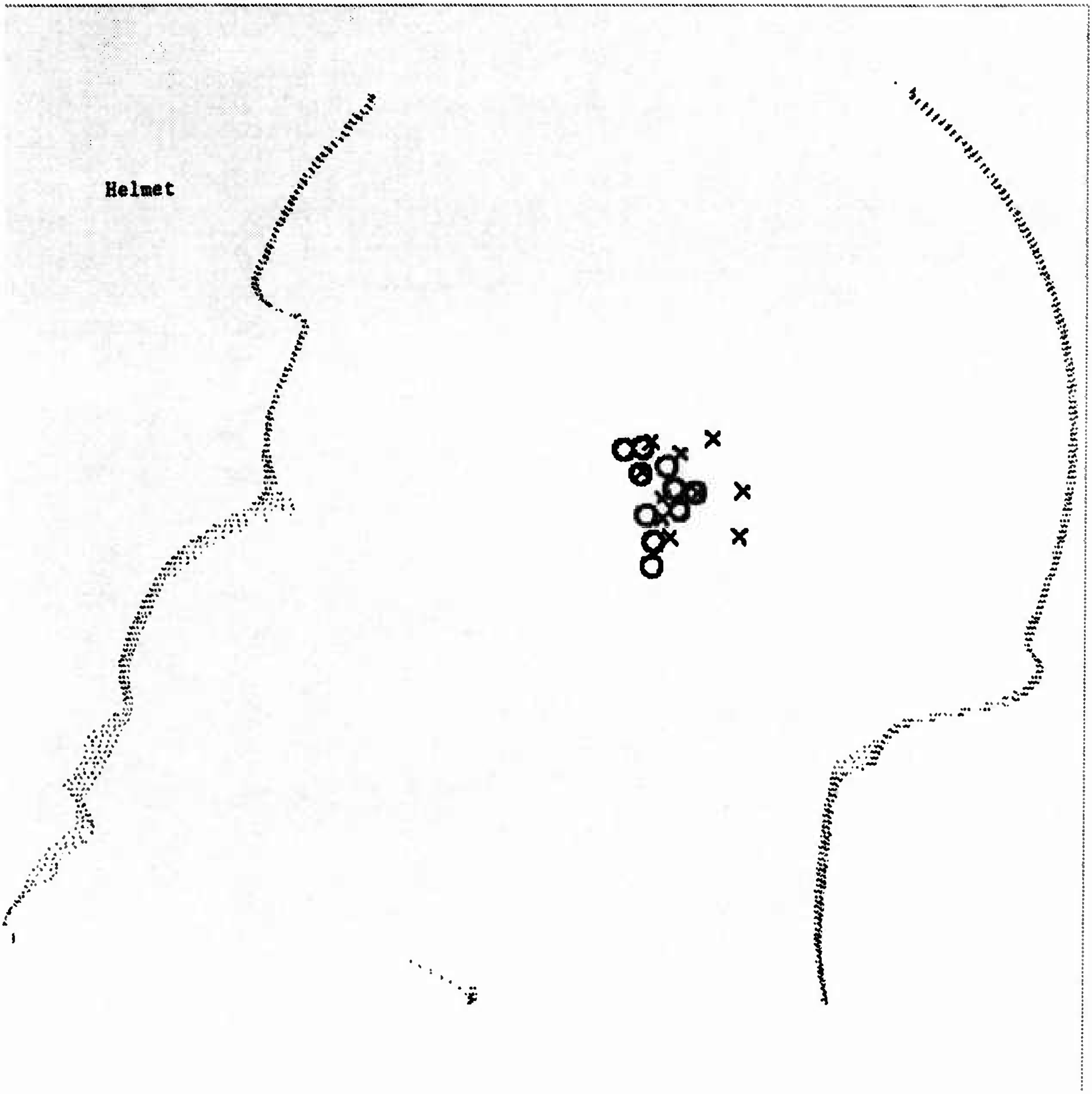

Figure 17. Ear regions for 10 subjects with respect to a size medium HGU 55/P

Figure 18. Surfaced scan within the HGU 55/P helmet.

REFERENCES

ASCC Air Standard 61/83, A Basis for Common Practices in the Conduct of Anthropometric Surveys, (Air Standardization Coordinating Committee), Washington DC, 1991.

Blackwell, S., I. Tebbetts, J. Crist, and G. Zehner., Head and Face Surface Anthropometry of USAF Aviators, Crew Systems Directorate, Human Engineering Division, Armstrong Laboratory, Wright-Patterson Air Force Base, OH (in press).

Cheverud, J.,Lewis, J.L. Banchrach, W., and Lew, W.E., "The measurement of form and variation in form:an application of three-dimensional quantitative morphology by finite-element methods," in American Journal of Physical Anthropology 62, 152-165, 1983.

Lele, Subhash and Joan T. Richtsmeier, "Euclidian distance matrix analysis: a coordinate free approach for comparing biological shapes using landmark data," in American Journal of Physical Anthropology, 86:415-427, 1991.

Simpson, R. E. Specimen Size Rolls for Aircrew Headgear Based on Analysis of the Head Measurement of 2000 Royal Air Force Aircrew. Technical Report 74072, Royal Aircraft Establishment, Farnborough, Hants, England, 1974.

Zeigen, Robert S., Milton Alexander, and Edmund Churchill. A Head Circumference Sizing System for Helmet Design. WADD TR 60-631, Wright Air Development Division, Wright-Patterson Air Force Base, Ohio, 1960. (AD 251939)

APPENDIX A
LANDMARK DESCRIPTIONS

The three-dimensional coordinates of a series of 32 anatomical landmarks were extracted from the surface scans. The landmarks chosen were those deemed to be commonly used. They were identified using a software routine which allows a person to point, with a cursor and a mouse, to a point of interest on the screen in order to record the point as a three-dimensional coordinate set. Twenty-four (24) of the points were pre-marked with dots before scanning, and the observers pointed to the center of the dots to record these points. These points are illustrated in Figure 19. The remaining 8 points were selected by judging the location from the screen image.

Descriptions of all 32 landmarks are found below. Those landmarks that do not fall in the center of the face were identified on both right and left sides.

Center of Pupil, right and left: the center of the pupil when the head is in the Frankfurt Plane and the subject is looking straight ahead; determined by visual inspection.

Chin: the most protruding point on the bottom edge of the chin, along the jawline; determined by visual inspection.

Euryon, right and left: the most widely separated points on the two sides of the skull; instrumentally determined.

Frontotemporale, right and left: the point of deepest indentation of the temporal crest of the frontal bone above the browridges; located by palpation.

Glabella: the most anterior point on the frontal bone midway between the bony browridges; determined by visual inspection and palpation.

Gonion, right and left: the most lateral point on the posterior angle of the mandible (jawbone); determined by palpation.

Inframalar, right and left: the most inferior point of the zygomatic process of the maxilla; determined by palpation.

Infraorbitale, right and left: the lowest point on the anterior border of the bony eye socket; determined by palpation.

Infrazygion, right and left: the inferior border of the zygomatic arch directly below zygion; determined by visual inspection and palpation.

Menton: the inferior point of the mandible in the midsagittal plane; determined by palpation.

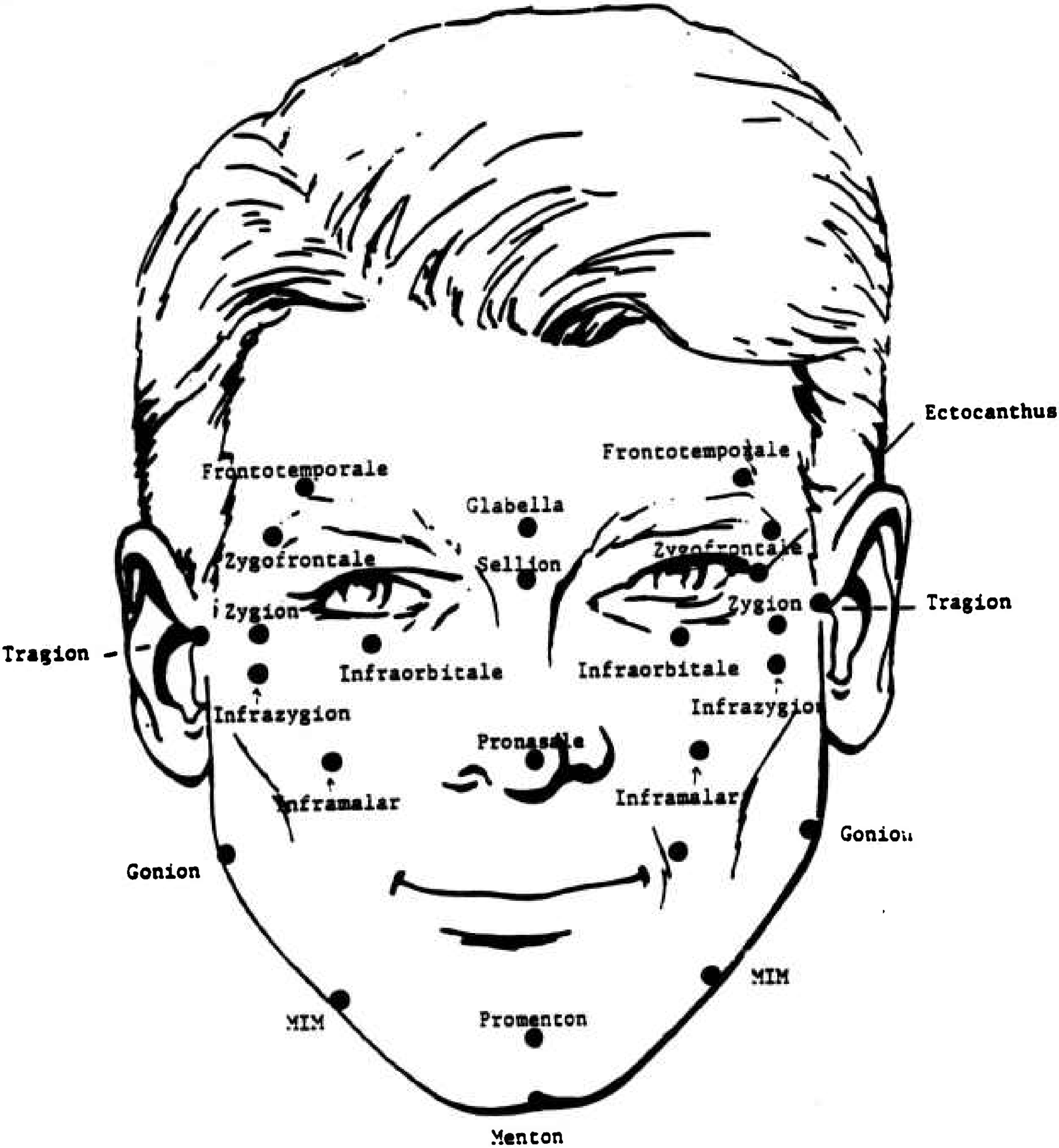

Figure 19. Pre-marked landmarks.

Midlateral Infra-Mandibular (MIM), right and left: the inferior lateral edge of the mandible midway between gonion and menton; determined by measurement and palpation.

Opisthocranion: the most posterior point on the skull; instrumentally determined.

Pronasale: the point of the most anterior projection of the tip of the nose in the midsagittal plane; located by visual inspection.

Promenton: the most anterior projection of the soft tissue of the chin in the midsagittal line; determined by visual inspection.

Sellion: the point of the deepest depression of the nasal bones at the top of the nose; determined by visual inspection and palpation.

Tragion, right and left: the superior point on the juncture of the cartilaginous flap (tragus) of the ear with the head; determined by visual inspection.

Submandibular: the point in the midsagittal plane where the lower jaw joins the neck; determined by visual inspection.

Subnasale: the point of intersection of the philtrum (groove of the upper lip) with the inferior surface of the nose, in the midsagittal plane; determined by visual inspection.

Top of Head: the highest point on the head, in a vertical plane from tragion when head is in the Frankfurt Plane; determined visually.

Zygion, right and left: the most lateral point on the zygomatic arch; instrumentally determined.

Zygofrontale, right and left: the most lateral point of the frontal bone where it forms the upper margin of the bony eye socket; determined by palpation.

APPENDIX B
TRADITIONAL MEASUREMENT DESCRIPTIONS

Bigonial Breadth: the distance between the right and left gonion landmarks; measured with a spreading calipers.

Bitragion Breadth: the distance between the right and left tragions; measured with a spreading caliper.

Bitragion-Chin Arc: the surface distance between right and left tragion across the anterior point of the chin; measured with a tape measure.

Bitragion-Coronal Arc: the surface distance between right tragion and left tragion across the top of the head; measured with a tape measure.

Bitragion-Frontal Arc: the surface distance between right and left tragion across the frontottemporale landmarks; measured with a tape measure.

Bitragion-Menton Arc: the surface distance between right and left tragion across menton landmark; measured with a tape measure.

Bitragion-Submandibular Arc: the surface distance between right and left tragion across the submandibular landmark at the junction of the jaw and neck; measured with a tape measure.

Bitragion-Subnasale Arc: the surface distance between right and left tragion across the bottom of the nose (subnasale); measured with a tape measure.

Bizygofrontale Breadth: the distance between the right and left zygofrontale landmarks; measured with a spreading caliper.

Bizygomatic Breadth: the greatest distance between the right and left zygofrontale landmarks; measured with a spreading caliper.

Glabella-Pronasale Length: the distance between the glabella landmark and pronasale landmark; measured with a sliding caliper.

Head Breadth: the maximum horizontal breadth of the head above the ears; measured with a spreading caliper.

Head Circumference: the maximum circumference of the head with the tape measure passing over glabella and above the ears.

Head Length: the distance in the midsagittal plane from the glabella landmark to the posterior point on the back of the head; measured with a spreading caliper.

Interpupillary Breadth: the distance between the center of the right pupil and the center of the left pupil; measured with a sliding caliper.

Interpupillary Distance: the distance between the center of the right pupil and the center of the left pupil; measured with a pupillometer.

Menton-Sellion Length: the distance between the menton and sellion landmarks with the subject's teeth lightly occluded; measured with a sliding caliper.

Minimum Frontal Breadth: the distance between the right and left frontotemporale landmarks; measured with a spreading caliper.

Tragion-Top of Head: the distance between right tragion and the top of the head at a point vertical from tragion when the subject is in the Frankfurt Horizontal position; measured with a beam caliper.

APPENDIX C
HALF SCALE PLOTS

The following are the half scale plots, described earlier, of the 16 subjects in four views, two views to a page. Each page has a scale on it at the bottom to assist in reconstructing the original size. Also the subject number is shown at the bottom of the left hand plot on each page.

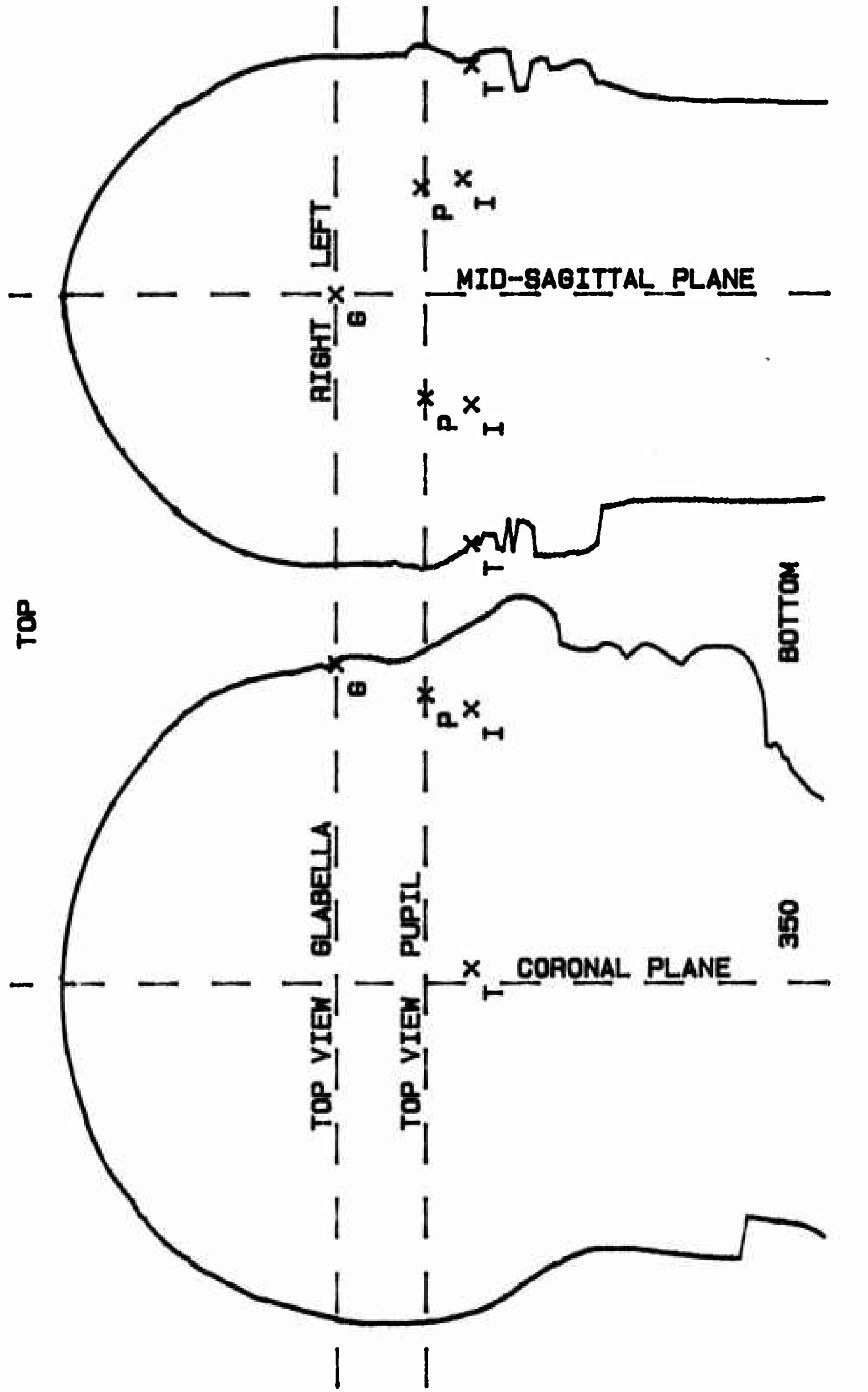

RIGHT SIDE VIEW (MID-SAGITTAL PLANE) FRONT VIEW (CORONAL PLANE)
(G) = GLABELLA (P) = PUPIL (T) = TRAGION (I) = INFRAORBITALE
0 — 10 - INCHES

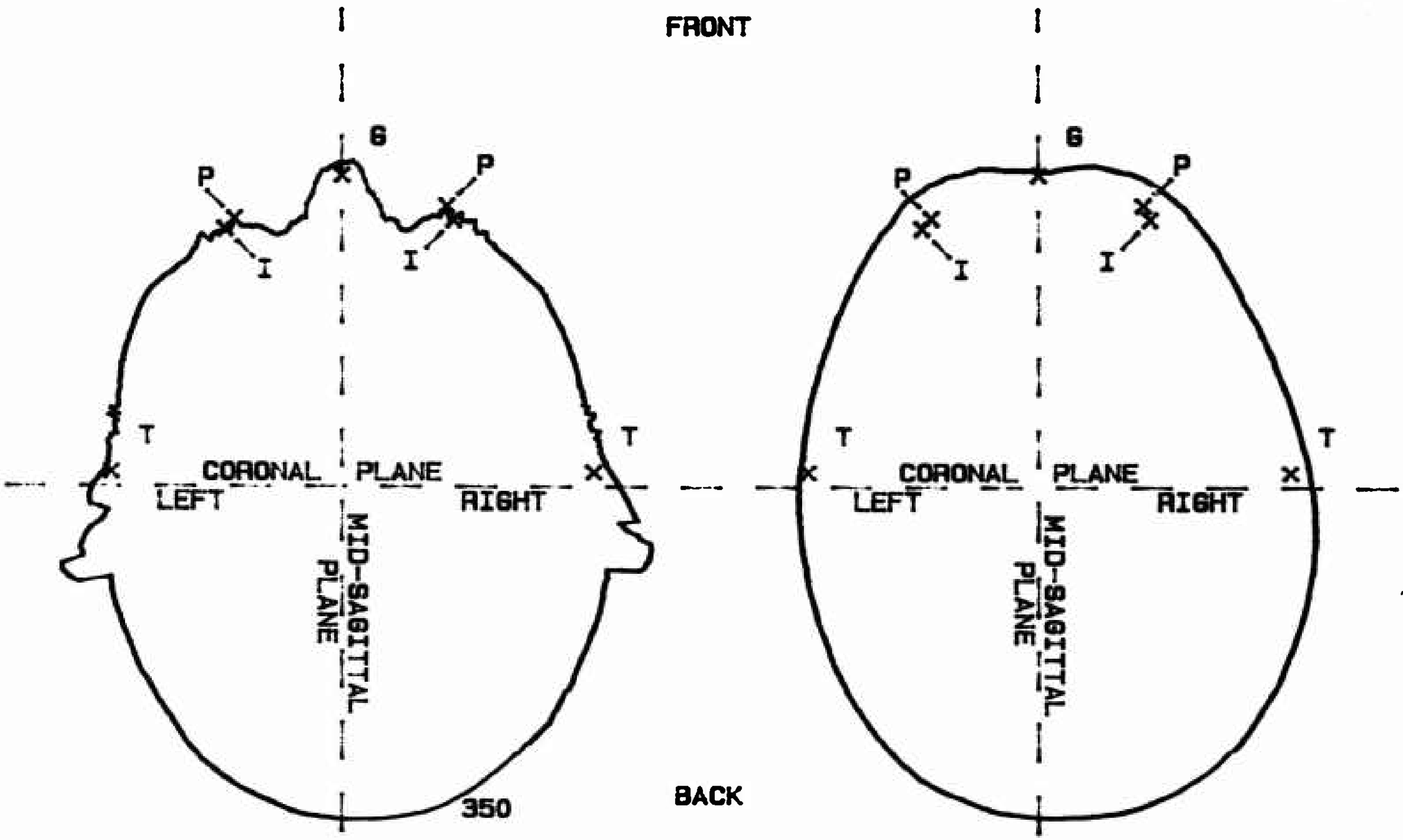

CROSS SECTION AT PUPIL CROSS SECTION AT GLABELLA

(G) = GLABELLA (P) = PUPIL (T) = TRAGION (I) = INFRAORBITALE

0 —— 10 - INCHES

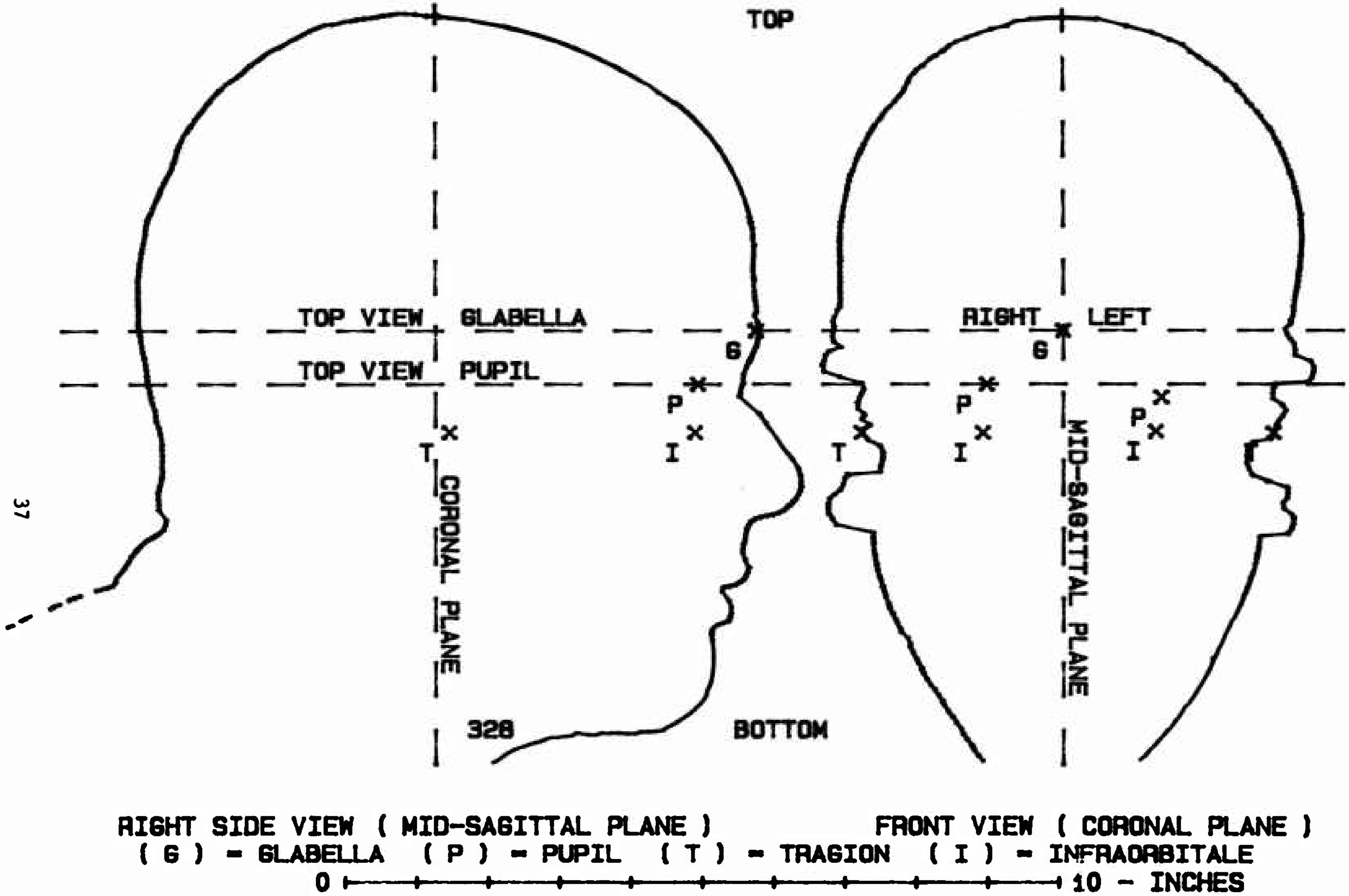

RIGHT SIDE VIEW (MID-SAGITTAL PLANE) FRONT VIEW (CORONAL PLANE)
(G) = GLABELLA (P) = PUPIL (T) = TRAGION (I) = INFRAORBITALE

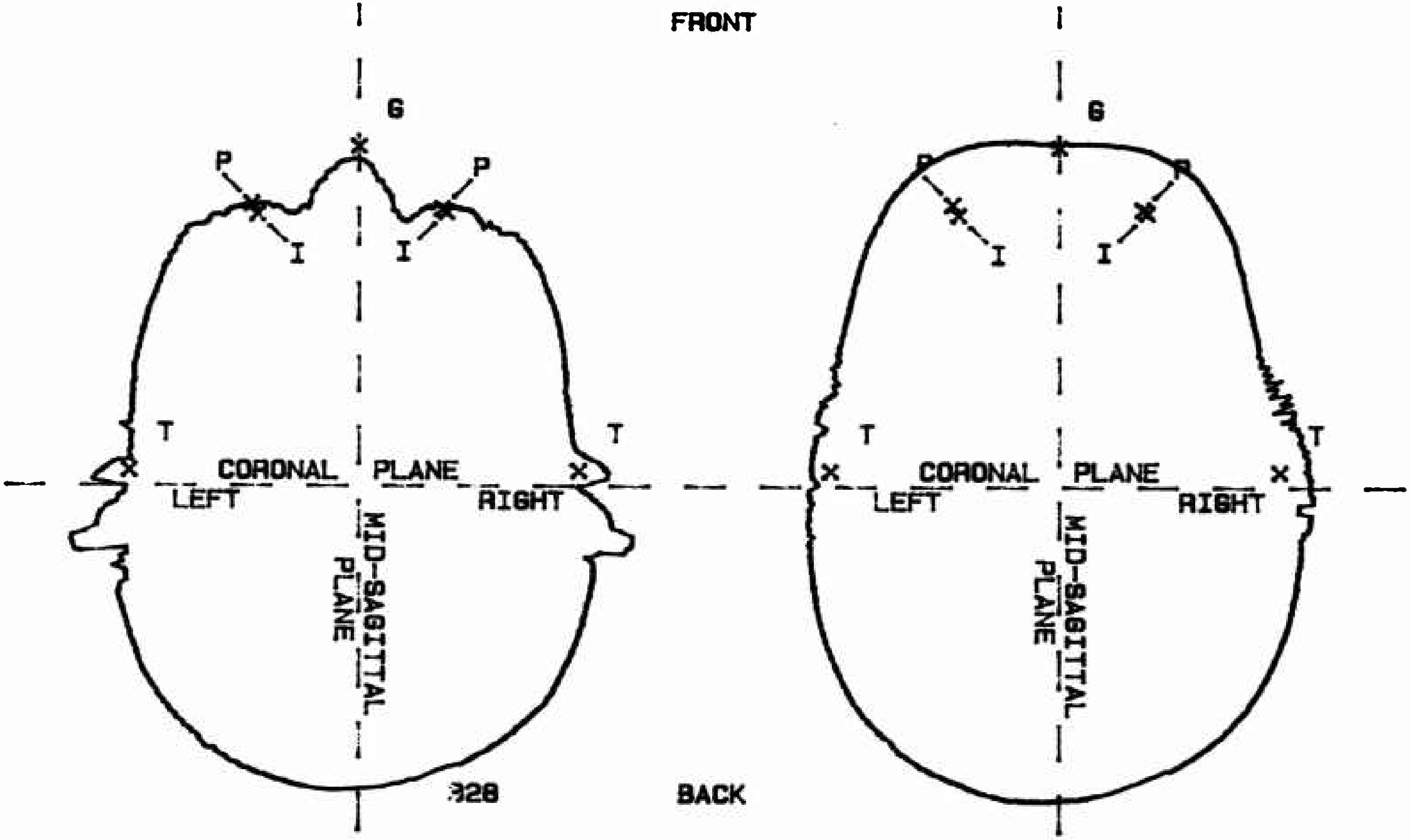

CROSS SECTION AT PUPIL

CROSS SECTION AT GLABELLA

(G) = GLABELLA (P) = PUPIL (T) = TRAGION (I) = INFRAORBITALE

0 — 10 - INCHES

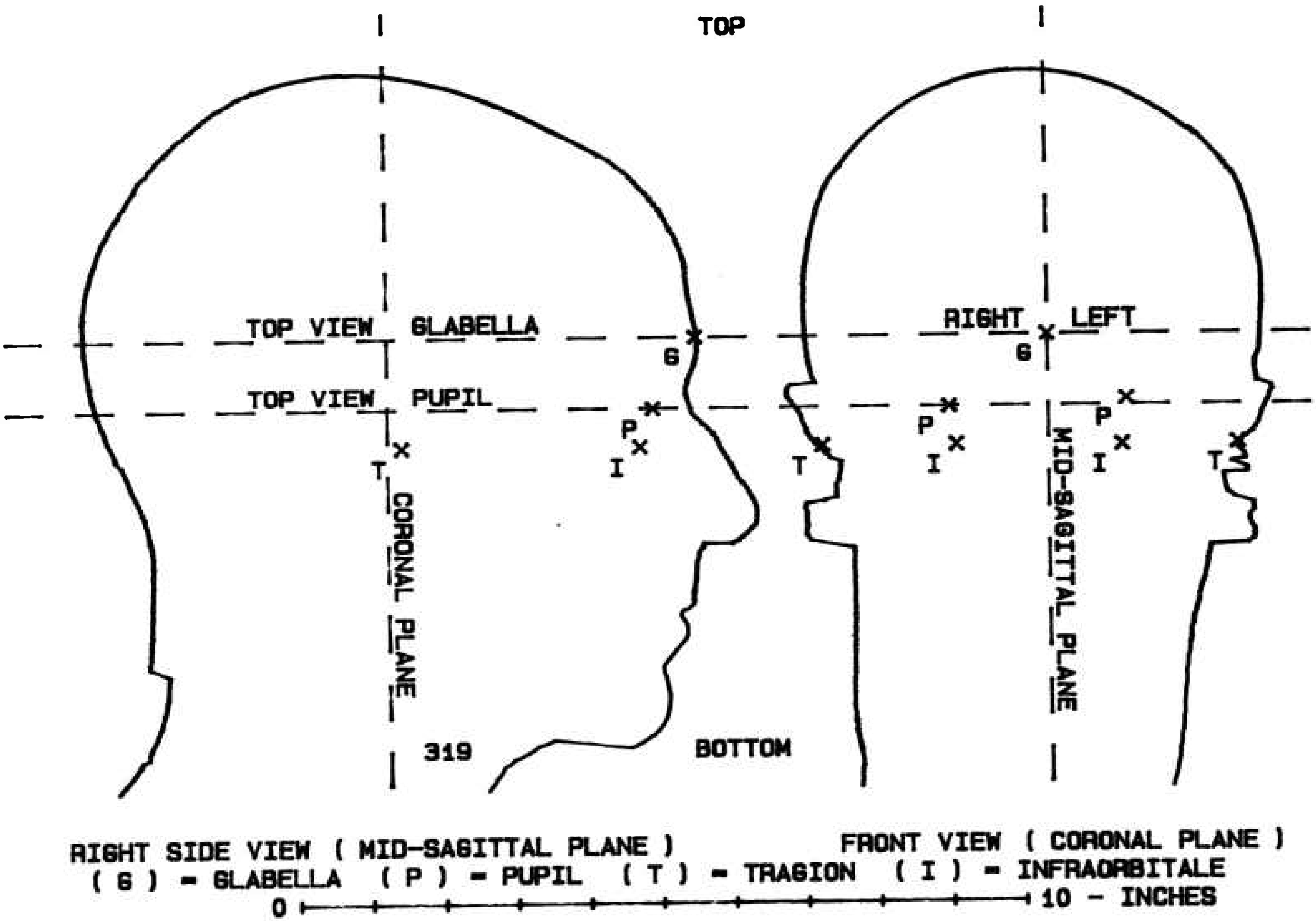
TOP
TOP VIEW GLABELLA
TOP VIEW PUPIL
G
P
I
T
CORONAL PLANE
319
BOTTOM
RIGHT LEFT
MID-SAGITTAL PLANE
RIGHT SIDE VIEW (MID-SAGITTAL PLANE)
FRONT VIEW (CORONAL PLANE)
(G) - GLABELLA (P) - PUPIL (T) - TRAGION (I) - INFRAORBITALE
0
10 - INCHES

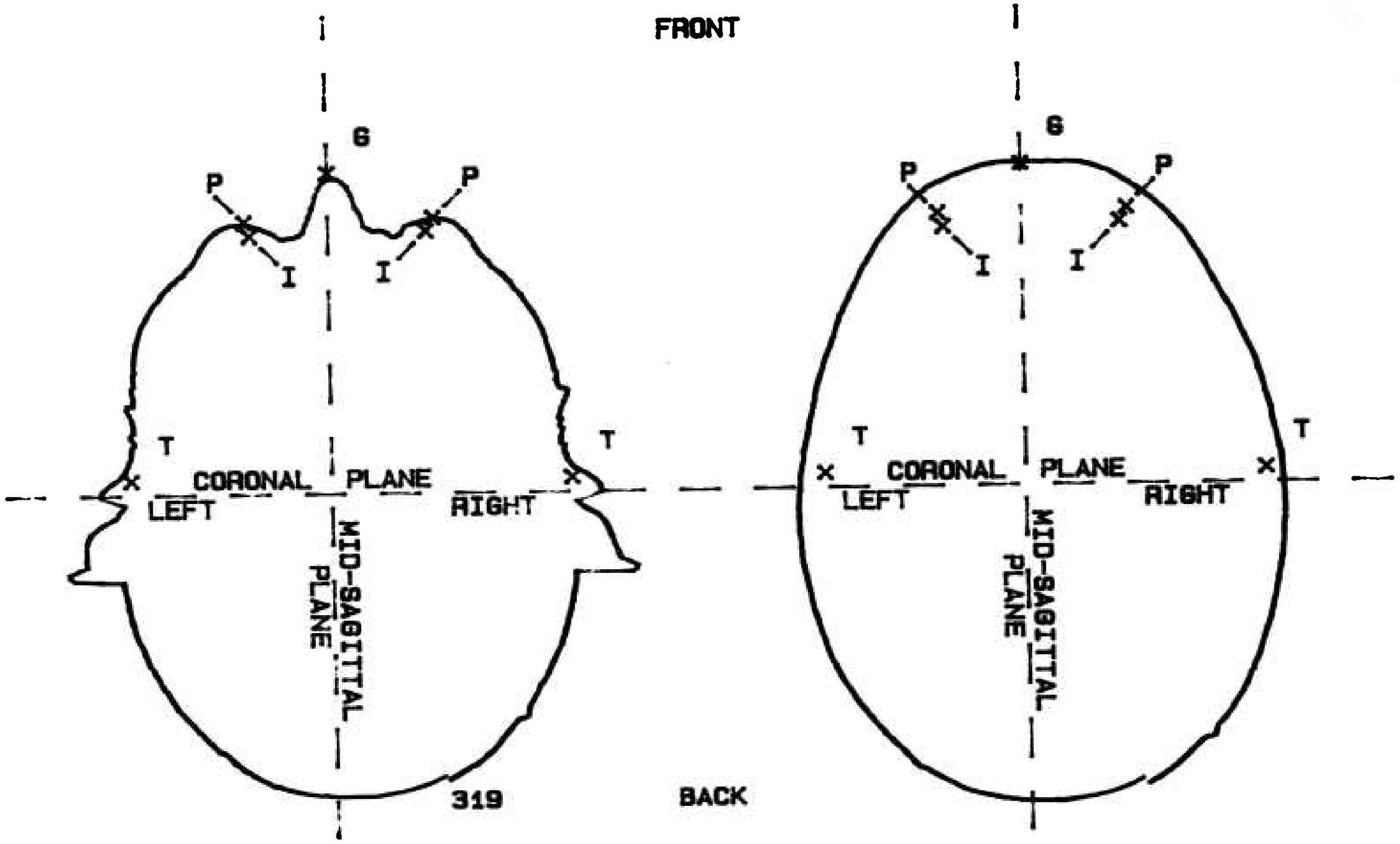

CROSS SECTION AT PUPIL

CROSS SECTION AT GLABELLA

(G) = GLABELLA (P) = PUPIL (T) = TRAGION (I) = INFRAORBITALE

0 — 10 - INCHES

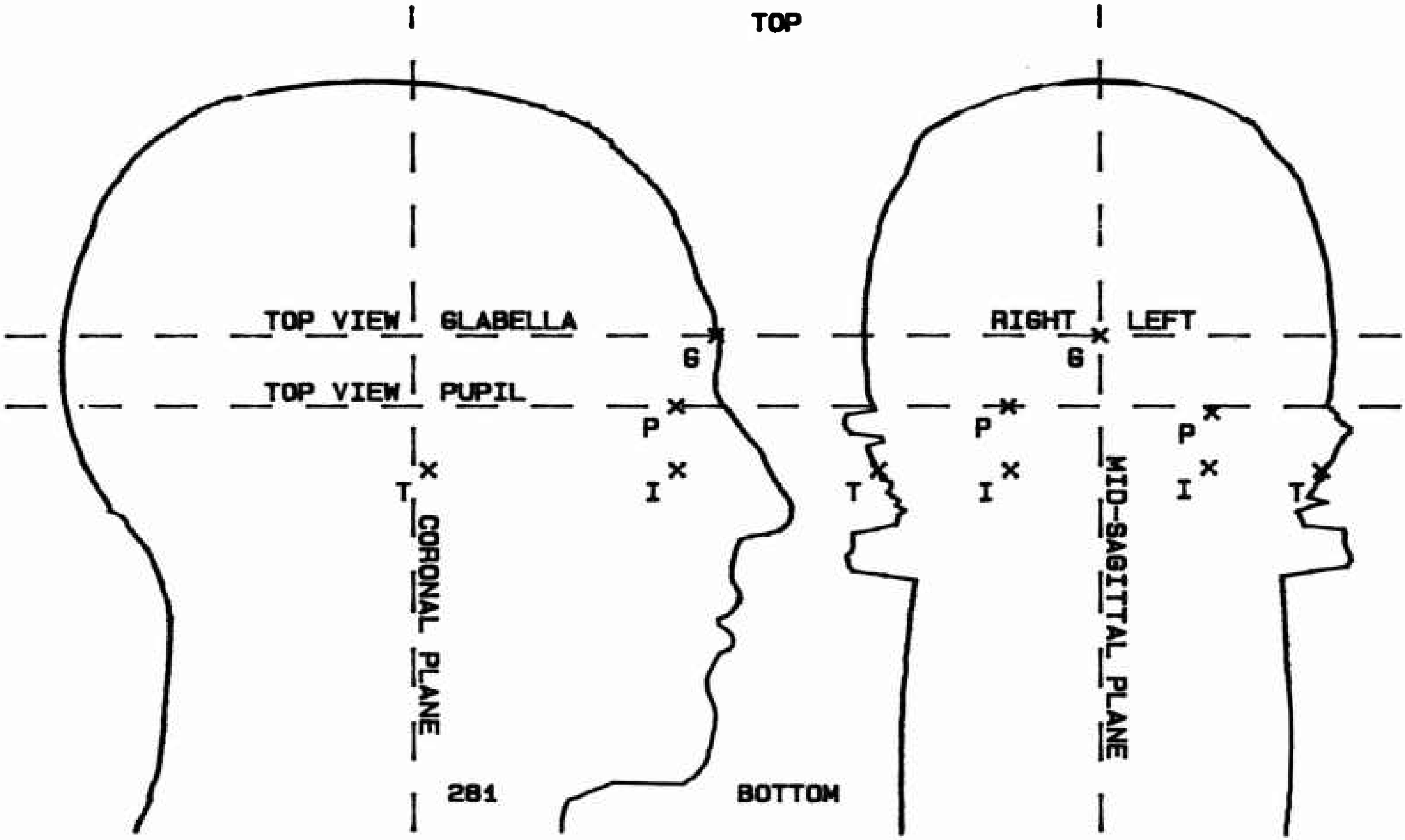

RIGHT SIDE VIEW (MID-SAGITTAL PLANE) FRONT VIEW (CORONAL PLANE)
(G) = GLABELLA (P) = PUPIL (T) = TRAGION (I) = INFRAORBITALE
0 ——— 10 - INCHES

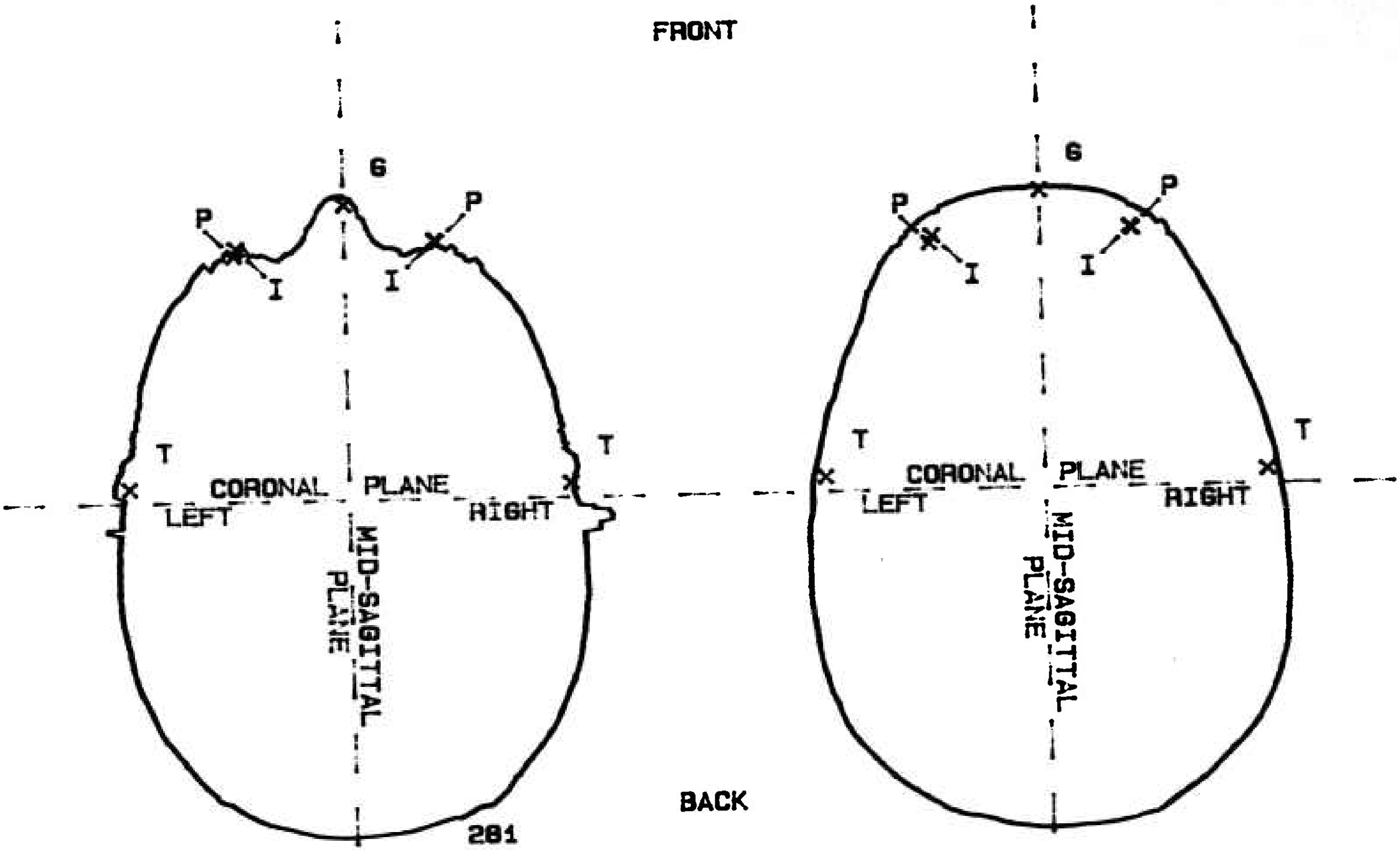

CROSS SECTION AT PUPIL

CROSS SECTION AT GLABELLA

(G) = GLABELLA (P) = PUPIL (T) = TRAGION (I) = INFRAORBITALE

0 — 10 - INCHES

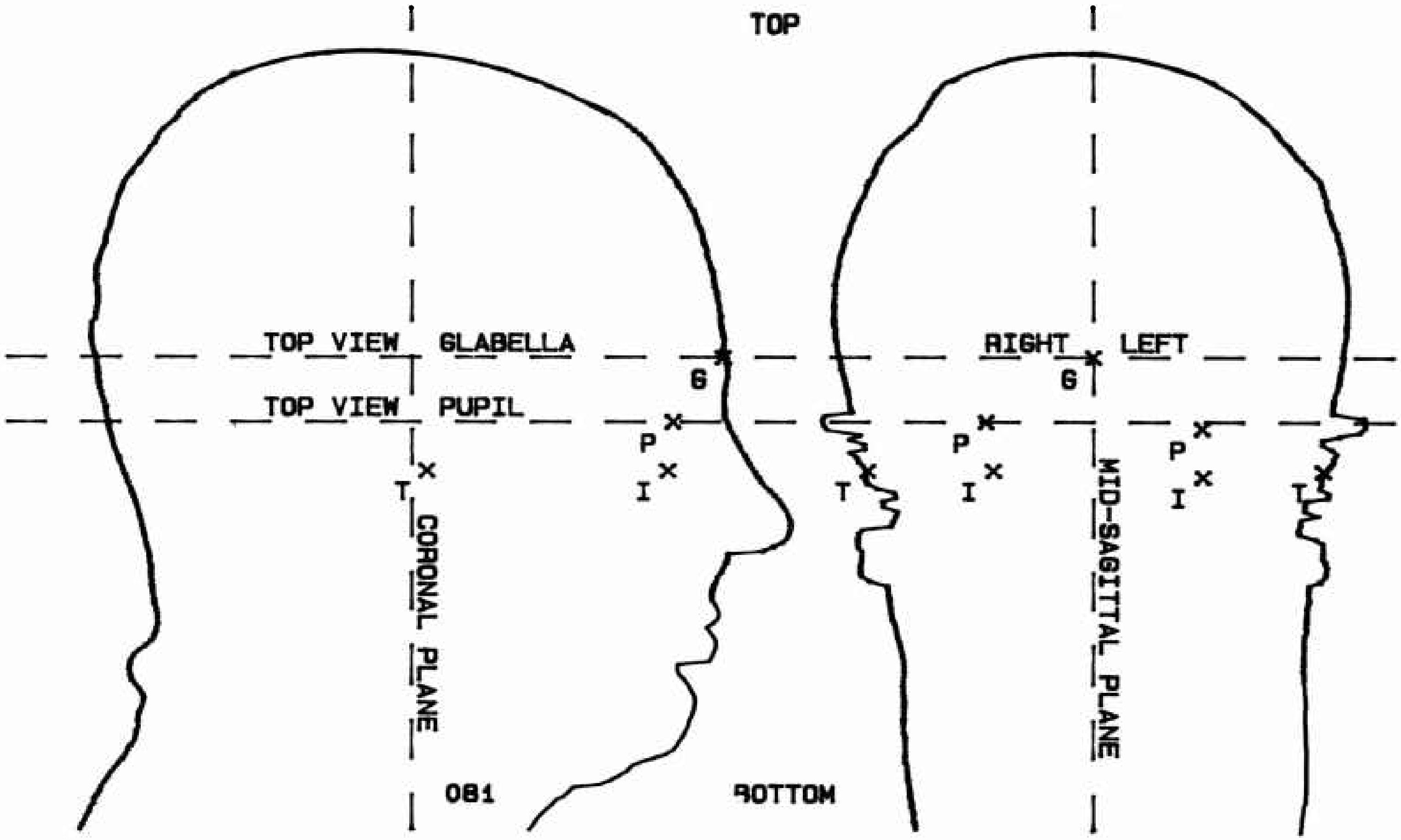

RIGHT SIDE VIEW (MID-SAGITTAL PLANE) FRONT VIEW (CORONAL PLANE)
(G) - GLABELLA (P) - PUPIL (T) - TRAGION (I) - INFRAORBITALE
0 —— 10 - INCHES

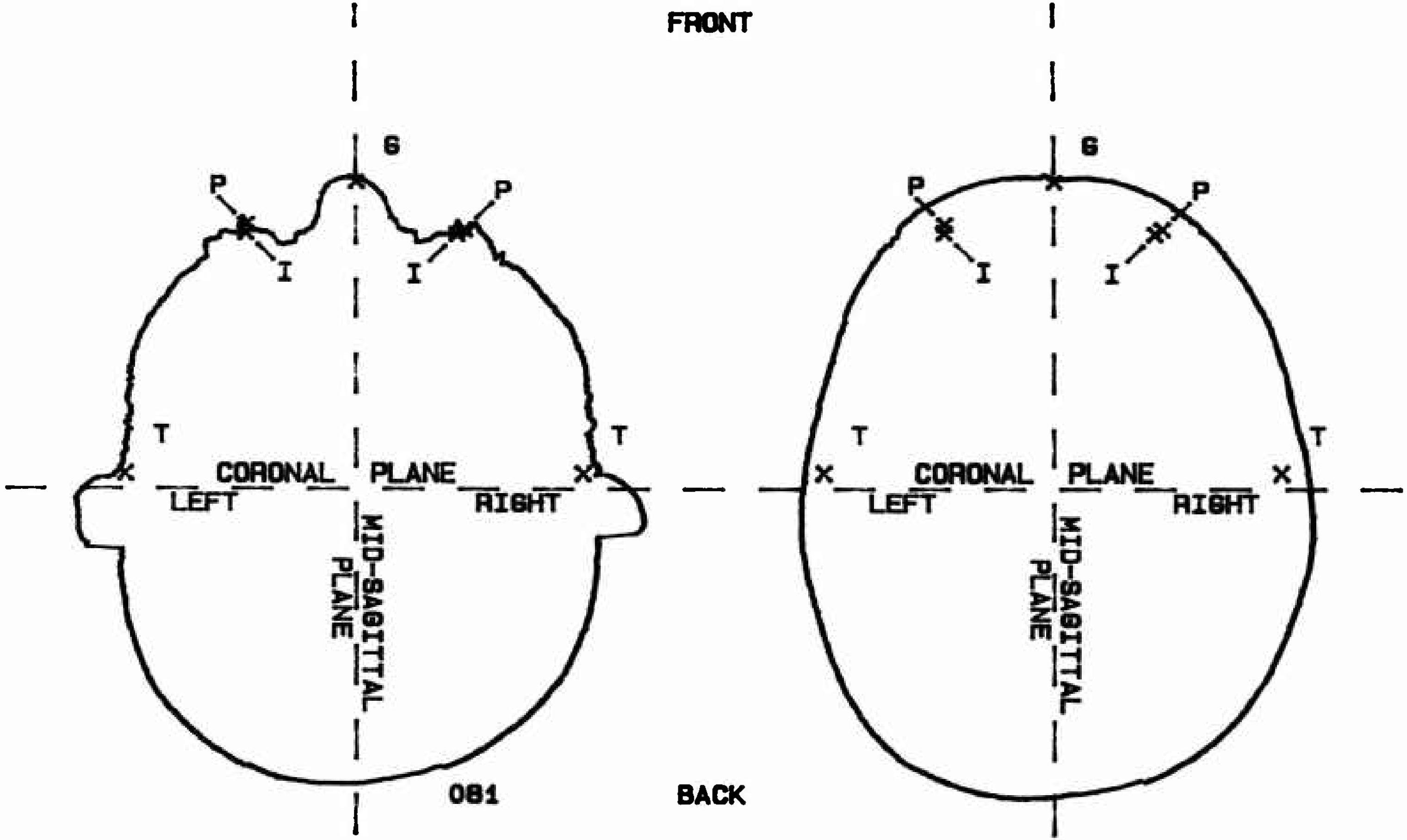

CROSS SECTION AT PUPIL　　CROSS SECTION AT GLABELLA

(G) = GLABELLA　(P) = PUPIL　(T) = TRAGION　(I) = INFRAORBITALE

0 — 10 - INCHES

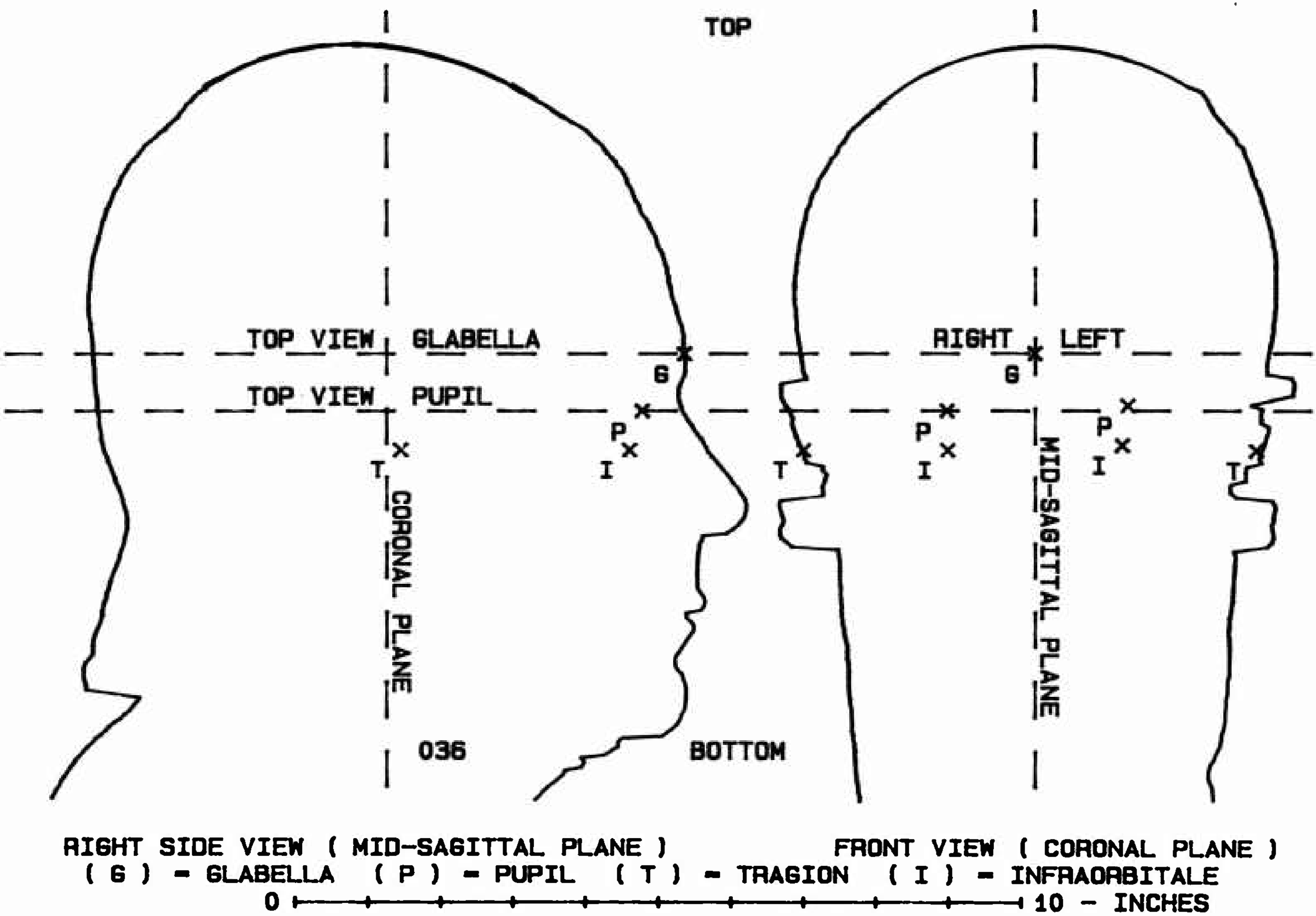

RIGHT SIDE VIEW (MID-SAGITTAL PLANE) FRONT VIEW (CORONAL PLANE)
(G) - GLABELLA (P) - PUPIL (T) - TRAGION (I) - INFRAORBITALE

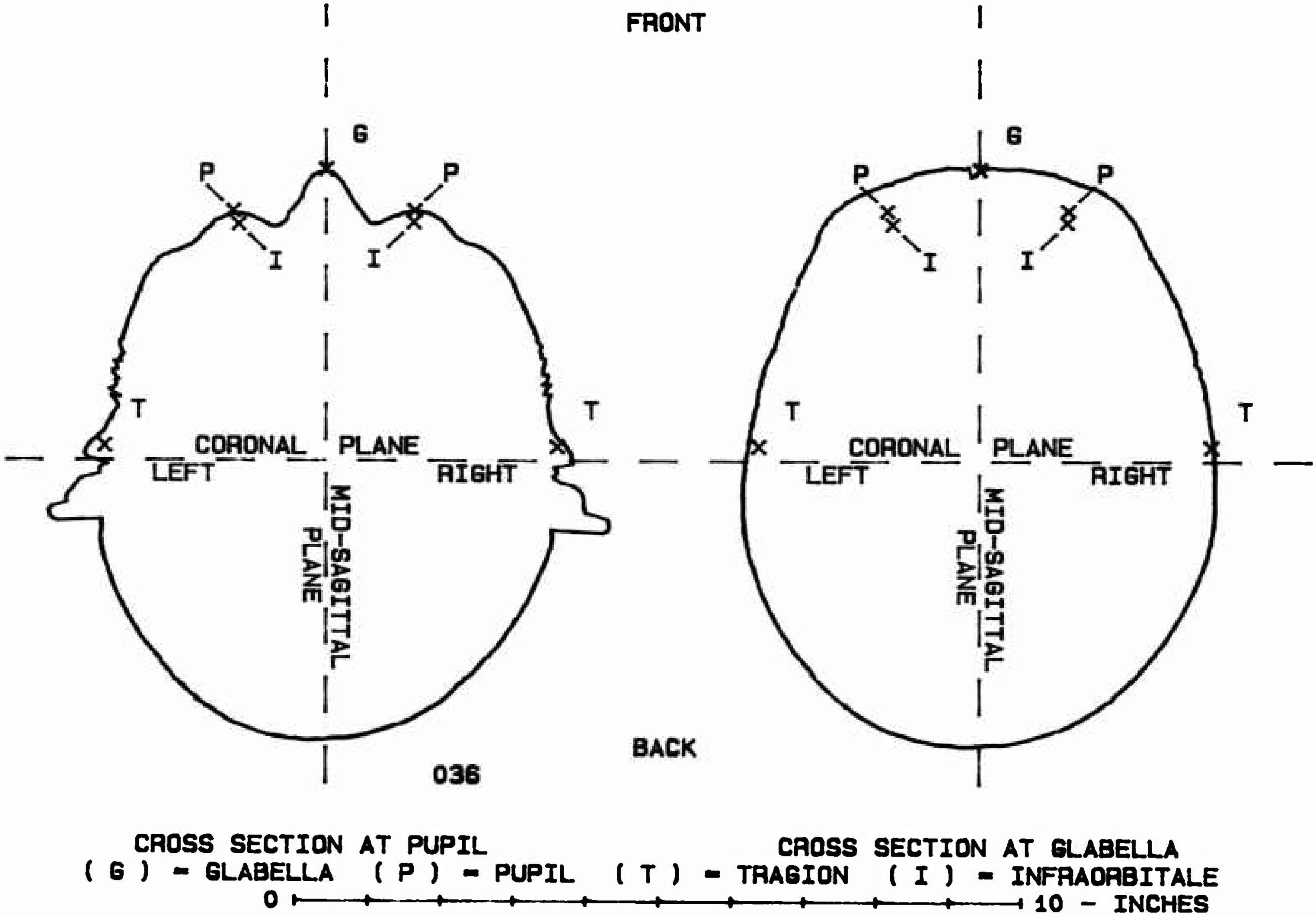

CROSS SECTION AT PUPIL

CROSS SECTION AT GLABELLA

(G) = GLABELLA (P) = PUPIL (T) = TRAGION (I) = INFRAORBITALE

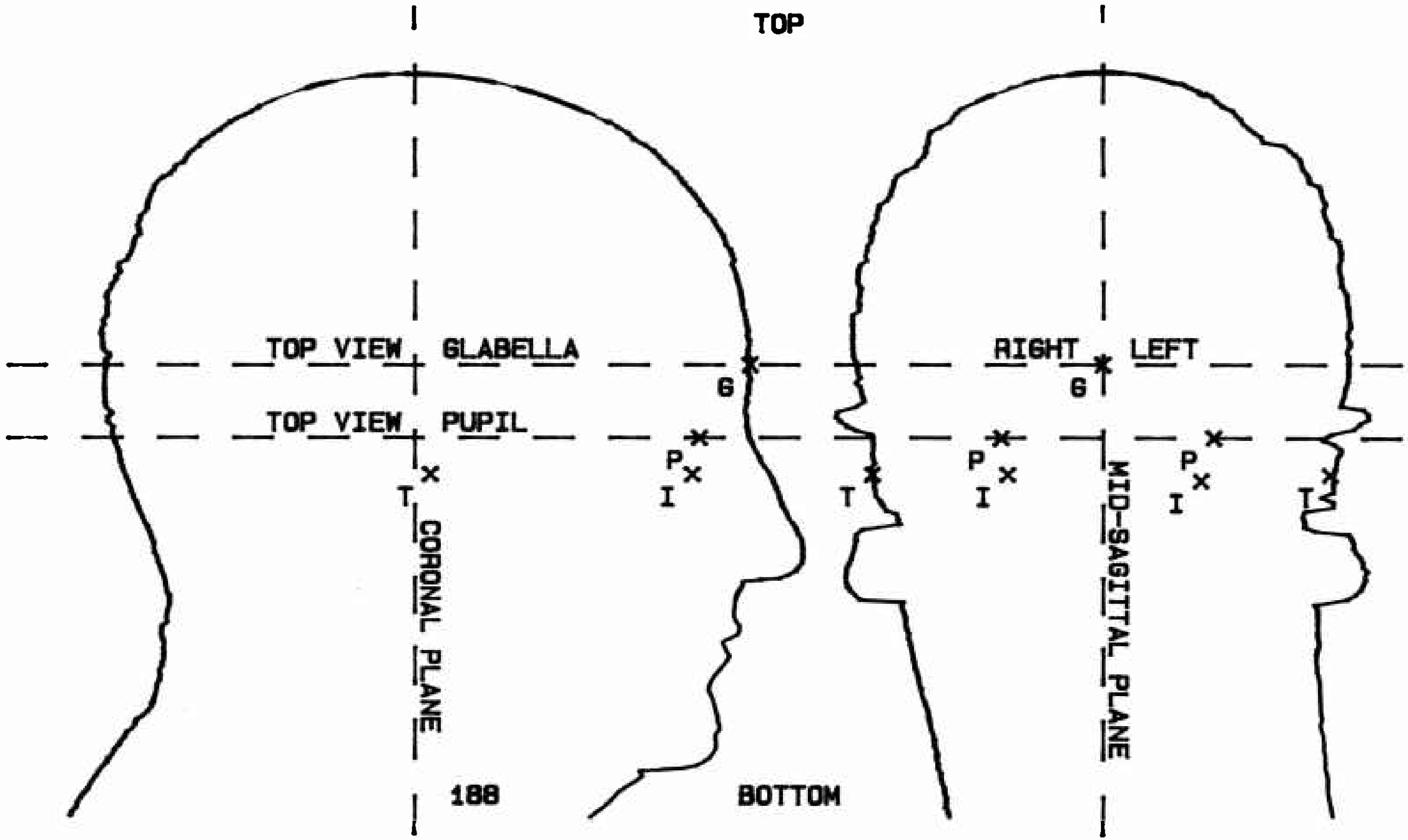

RIGHT SIDE VIEW (MID-SAGITTAL PLANE) FRONT VIEW (CORONAL PLANE)
(G) = GLABELLA (P) = PUPIL (T) = TRAGION (I) = INFRAORBITALE
0 — 10 - INCHES

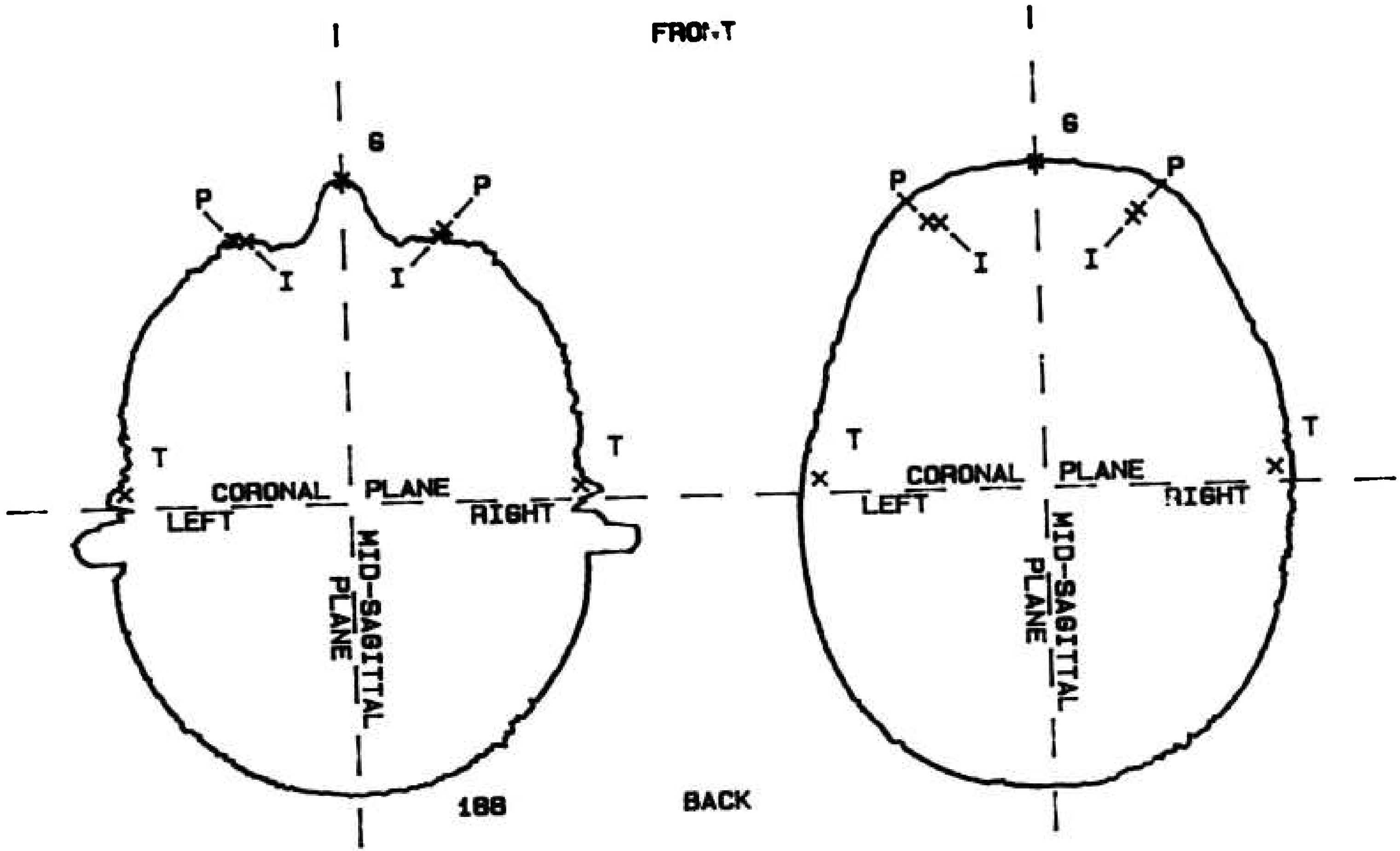

CROSS SECTION AT PUPIL

CROSS SECTION AT GLABELLA

(G) = GLABELLA (P) = PUPIL (T) = TRAGION (I) = INFRAORBITALE

0 — 10 - INCHES

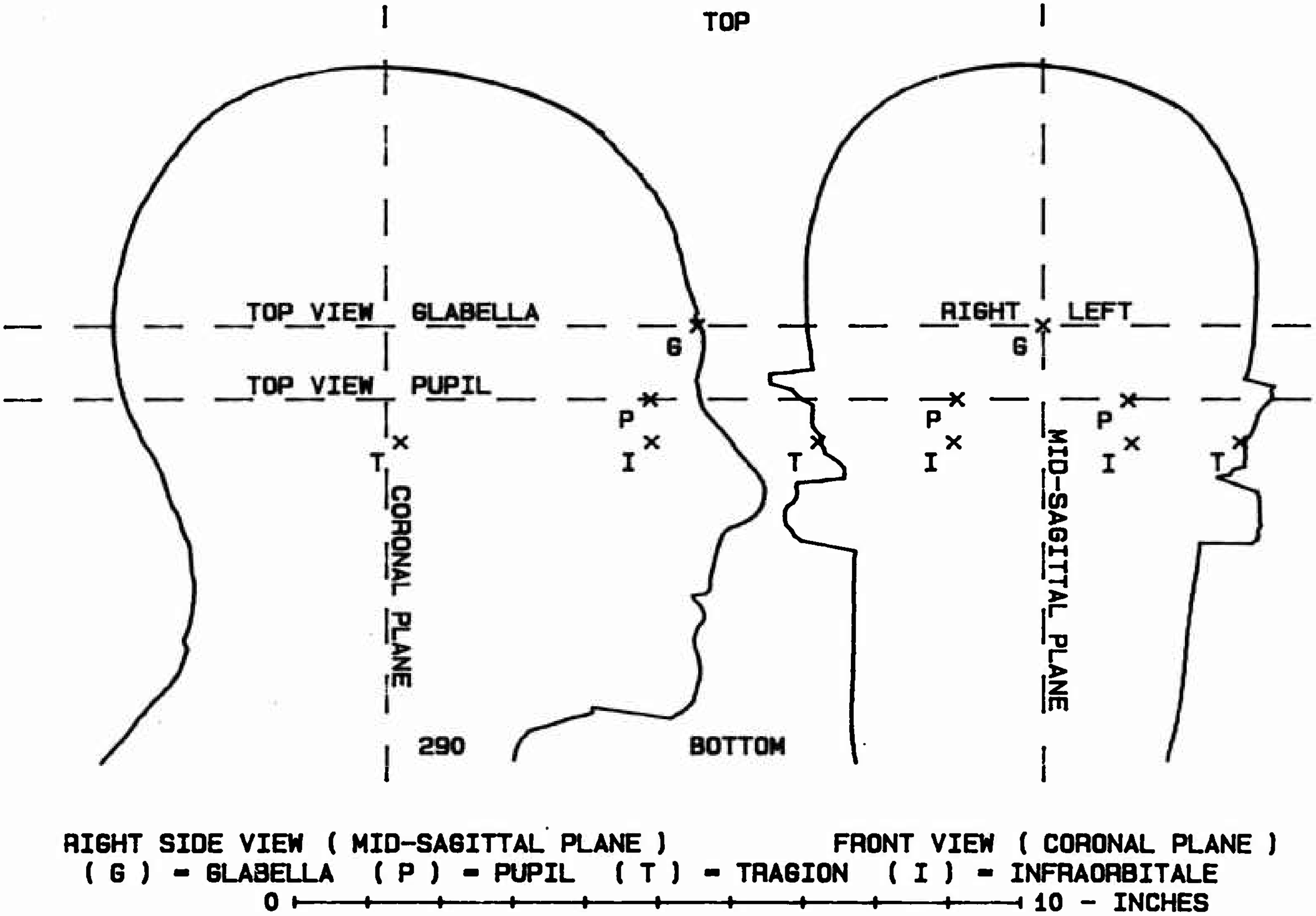

RIGHT SIDE VIEW (MID-SAGITTAL PLANE) FRONT VIEW (CORONAL PLANE)
(G) = GLABELLA (P) = PUPIL (T) = TRAGION (I) = INFRAORBITALE

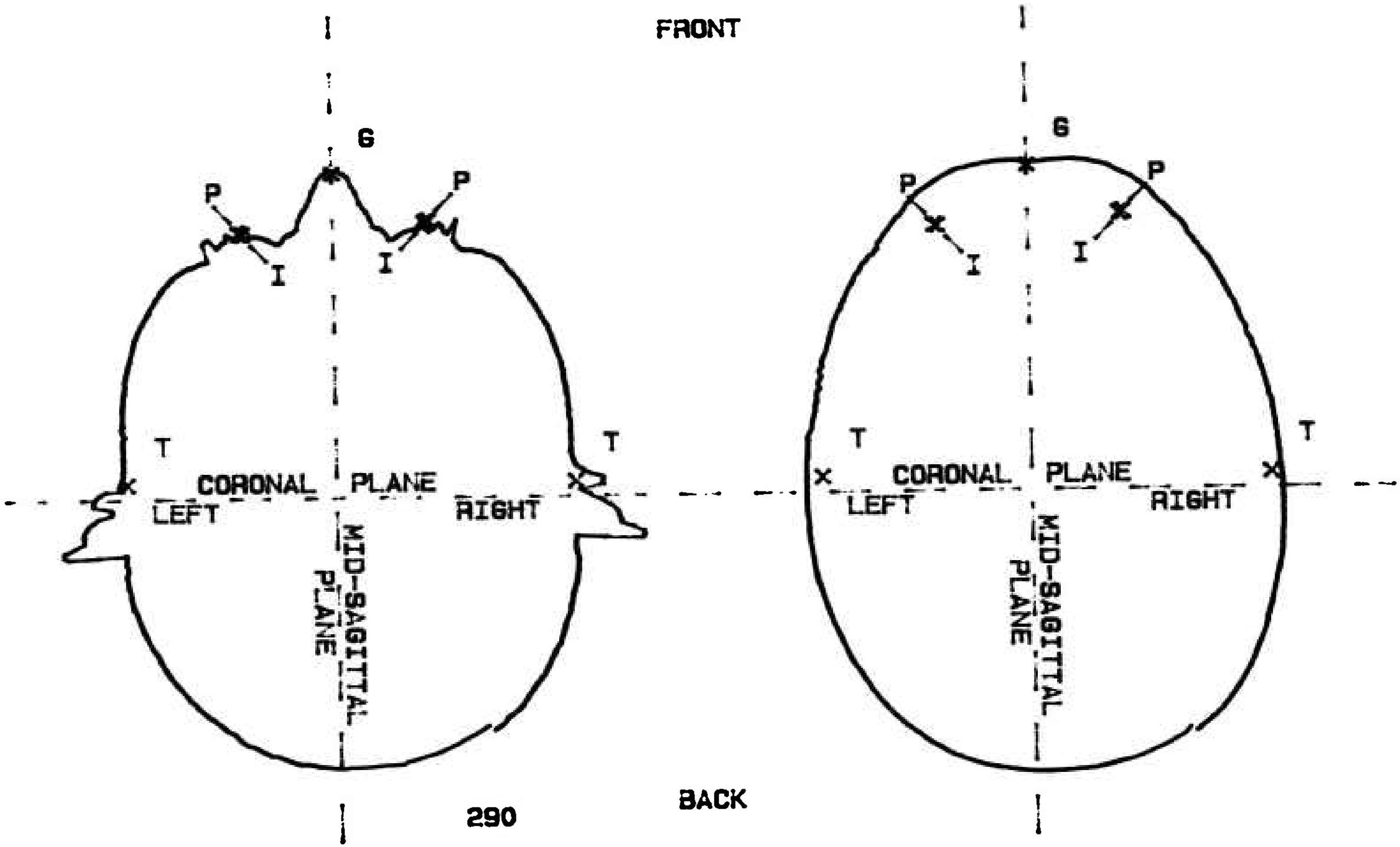

CROSS SECTION AT PUPIL

CROSS SECTION AT GLABELLA

(G) = GLABELLA (P) = PUPIL (T) = TRAGION (I) = INFRAORBITALE

0 ⊢ 10 – INCHES

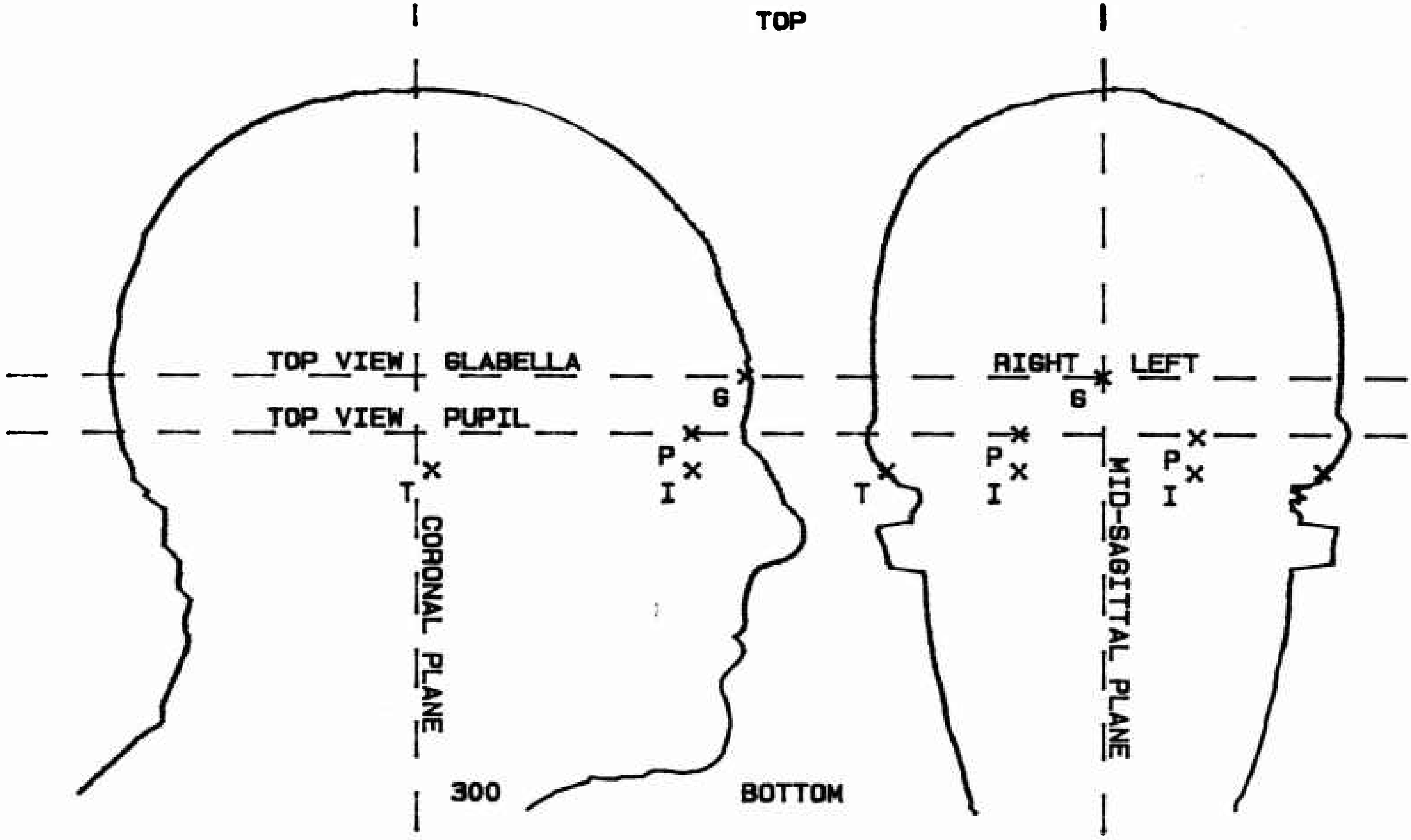

RIGHT SIDE VIEW (MID-SAGITTAL PLANE) FRONT VIEW (CORONAL PLANE)

(G) = GLABELLA (P) = PUPIL (T) = TRAGION (I) = INFRAORBITALE

0 —— 10 - INCHES

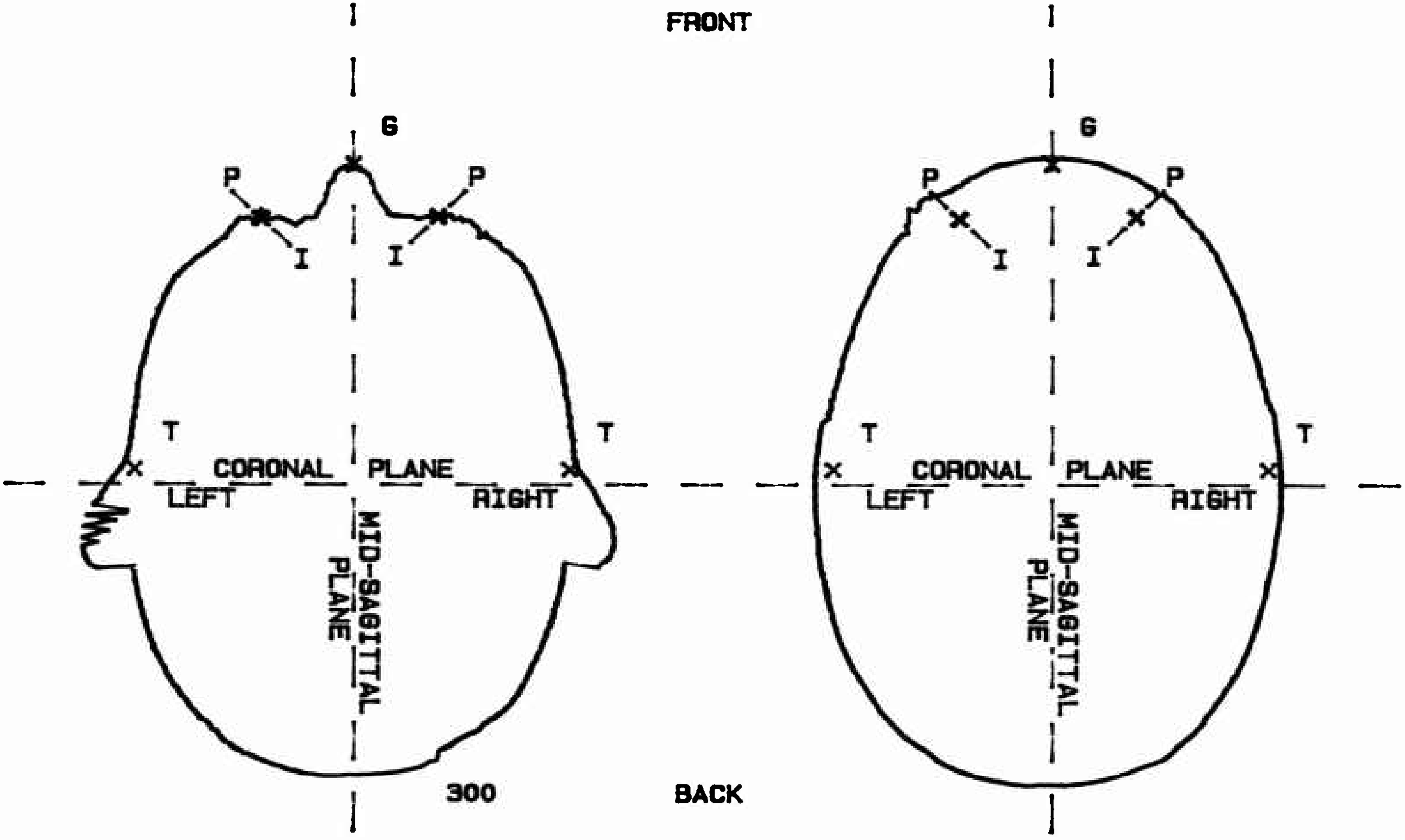

CROSS SECTION AT PUPIL CROSS SECTION AT GLABELLA

(G) = GLABELLA (P) = PUPIL (T) = TRAGION (I) = INFRAORBITALE

0 — 10 - INCHES

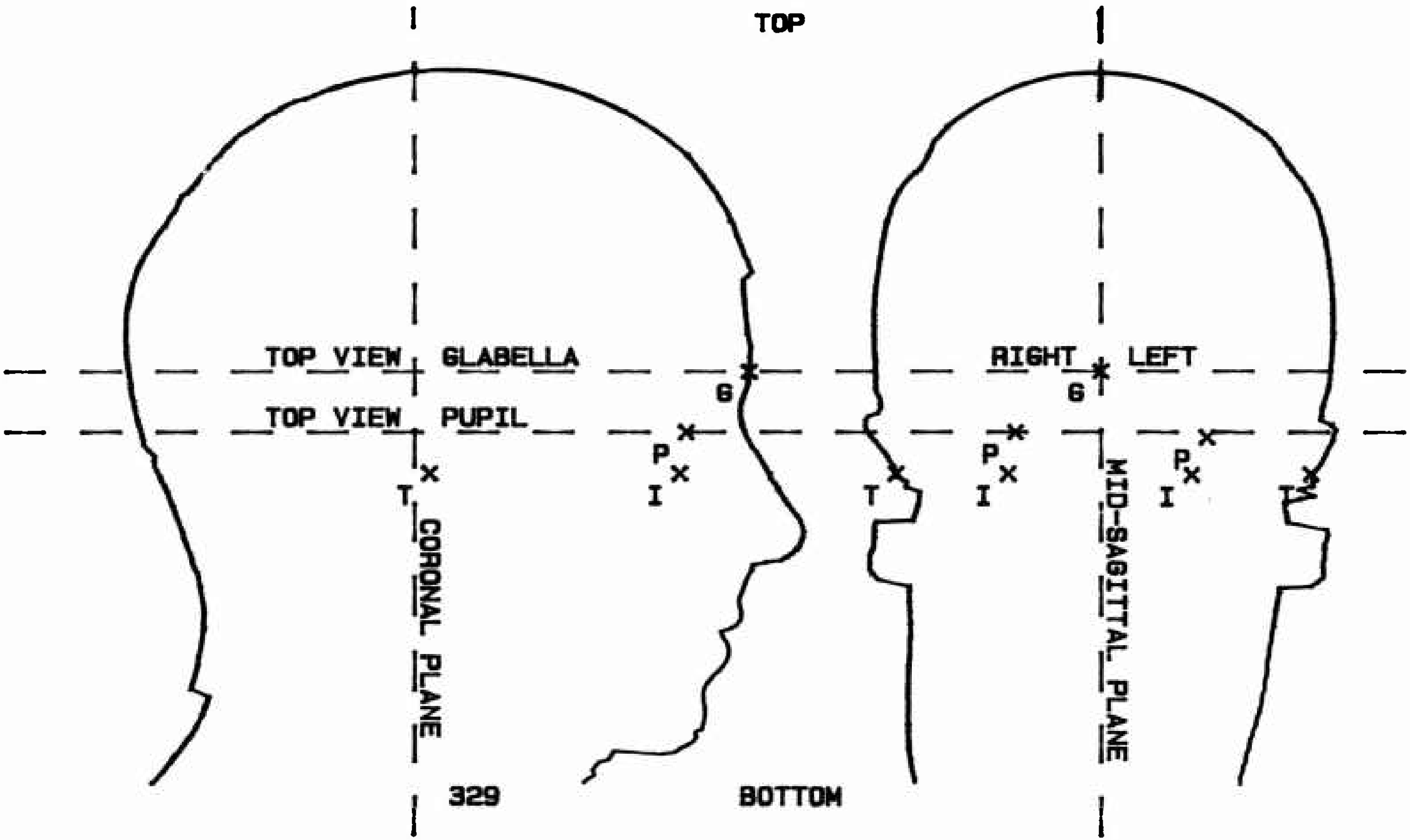

RIGHT SIDE VIEW (MID-SAGITTAL PLANE) FRONT VIEW (CORONAL PLANE)
(G) - GLABELLA (P) - PUPIL (T) - TRAGION (I) - INFRAORBITALE
0 —— 10 - INCHES

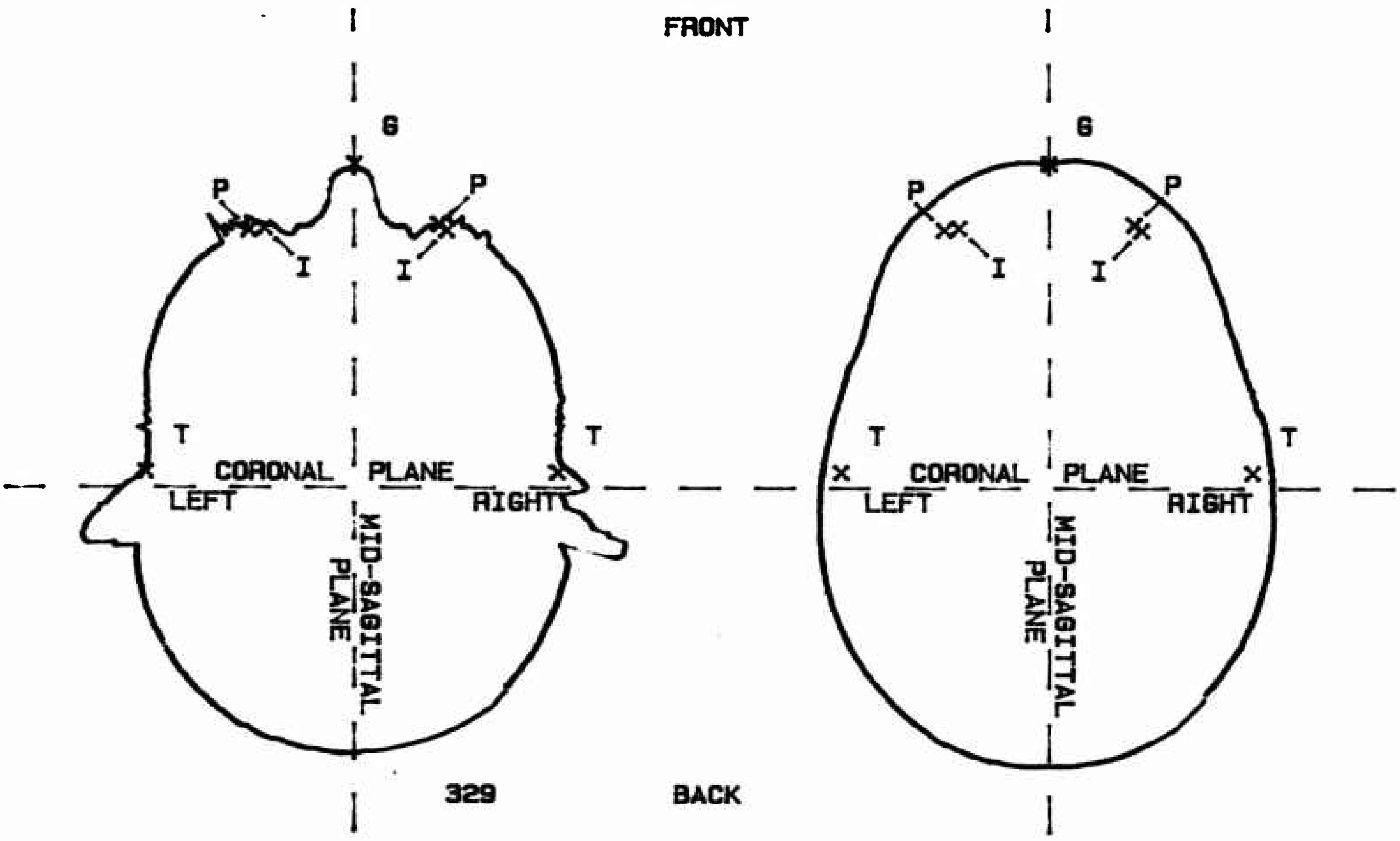

CROSS SECTION AT PUPIL   CROSS SECTION AT GLABELLA

(G) = GLABELLA (P) = PUPIL (T) = TRAGION (I) = INFRAORBITALE

0 ——— 10 - INCHES

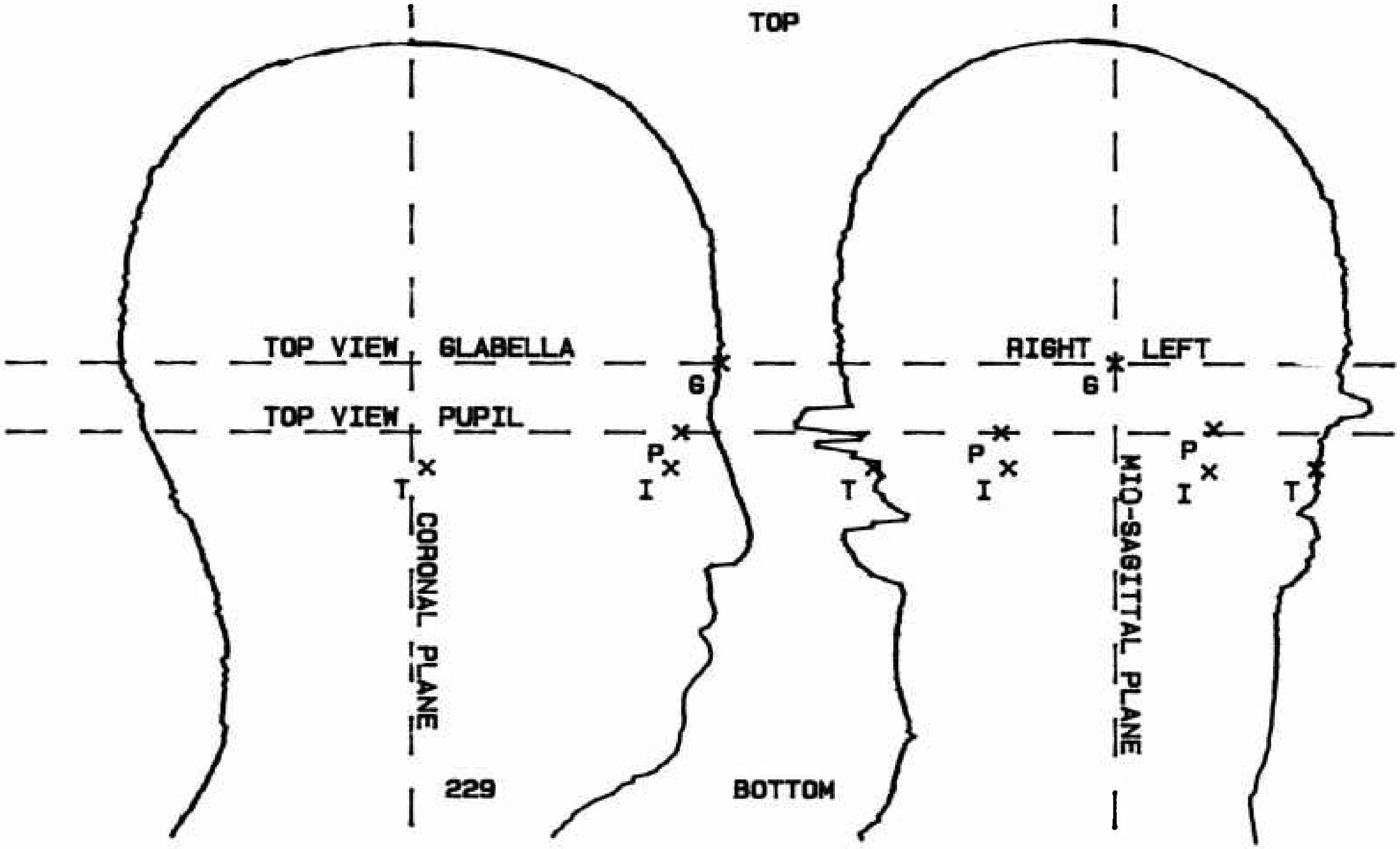

RIGHT SIDE VIEW (MID-SAGITTAL PLANE) FRONT VIEW (CORONAL PLANE)
(G) = GLABELLA (P) = PUPIL (T) = TRAGION (I) = INFRAORBITALE
0 —— 10 - INCHES

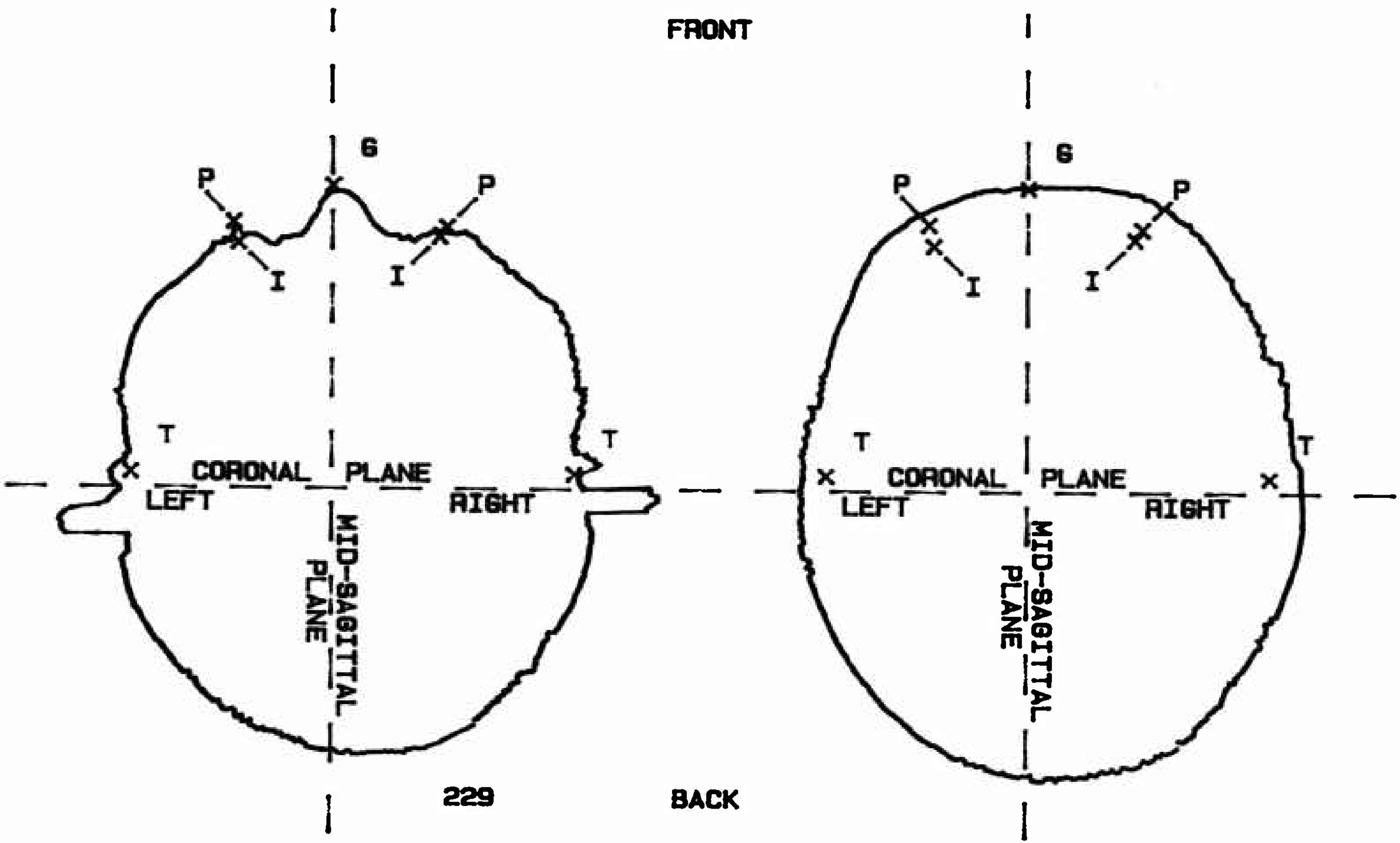

CROSS SECTION AT PUPIL

CROSS SECTION AT GLABELLA

(G) = GLABELLA (P) = PUPIL (T) = TRAGION (I) = INFRAORBITALE

0 — 10 - INCHES

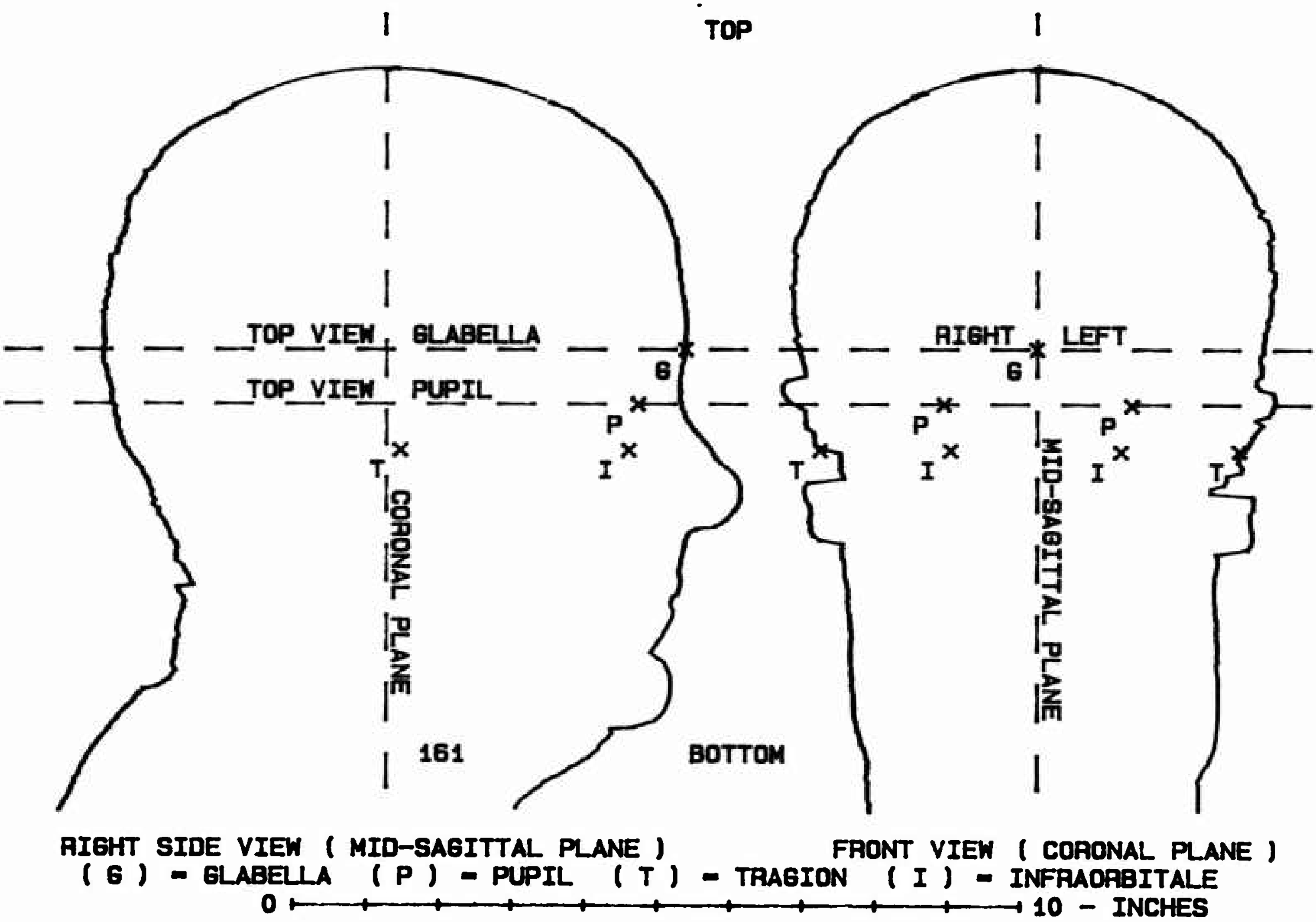
TOP
TOP VIEW GLABELLA
TOP VIEW PUPIL
CORONAL PLANE
G
P
I
T
161
BOTTOM
RIGHT LEFT
MID-SAGITTAL PLANE
RIGHT SIDE VIEW (MID-SAGITTAL PLANE)
FRONT VIEW (CORONAL PLANE)
(G) = GLABELLA (P) = PUPIL (T) = TRAGION (I) = INFRAORBITALE
0
10 - INCHES

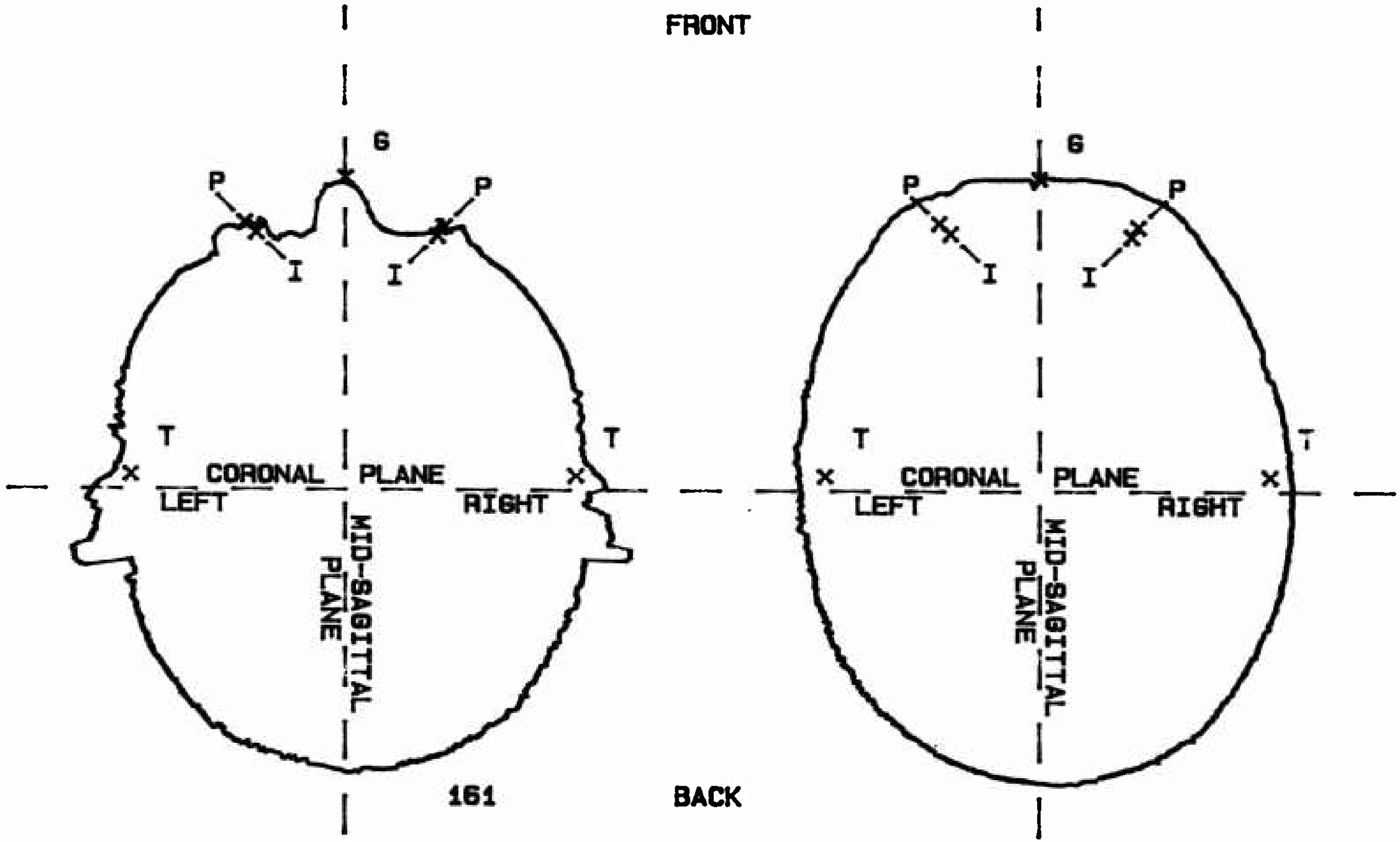

CROSS SECTION AT PUPIL CROSS SECTION AT GLABELLA

(G) - GLABELLA (P) - PUPIL (T) - TRAGION (I) - INFRAORBITALE

0 —— 10 - INCHES

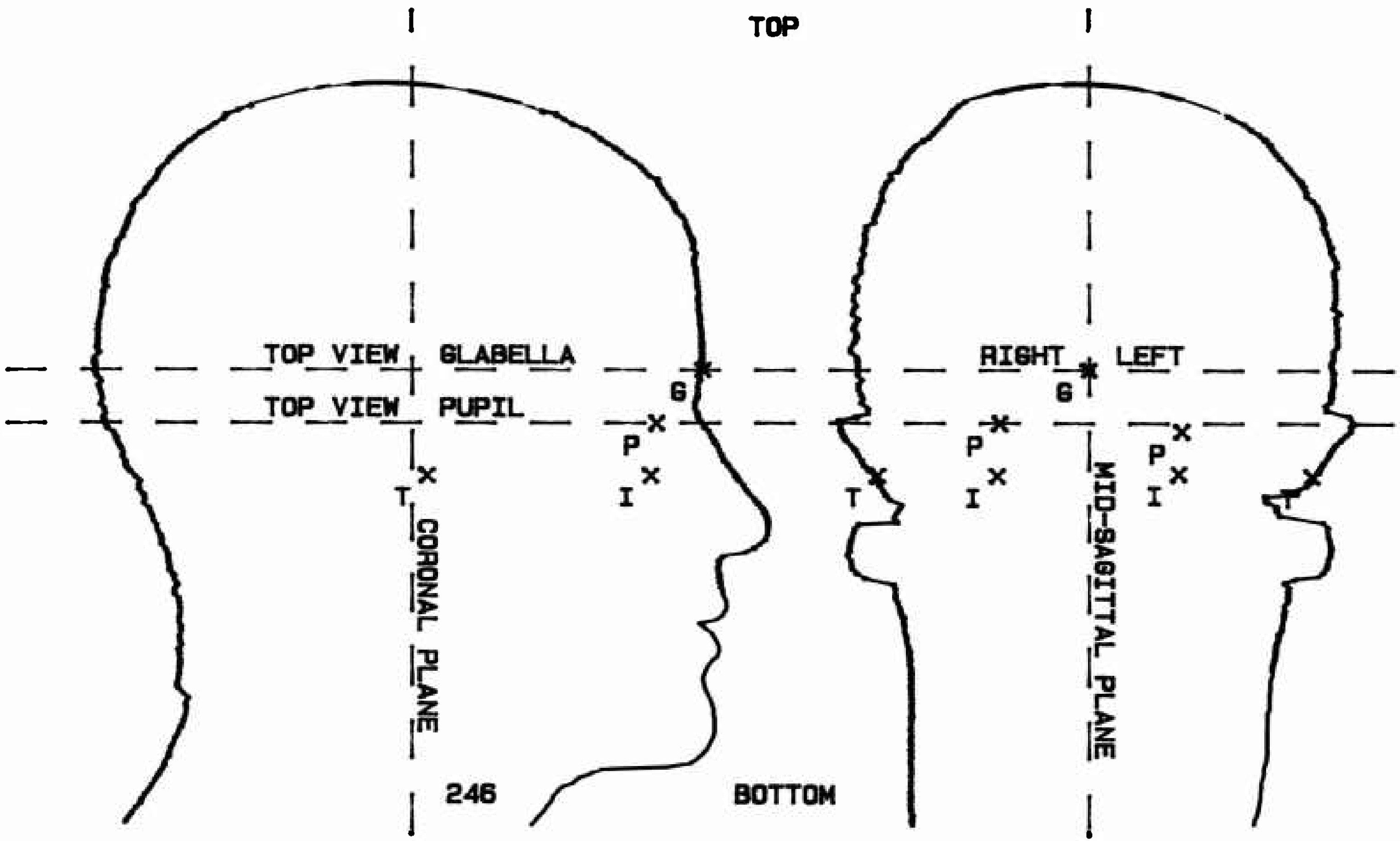

RIGHT SIDE VIEW (MID-SAGITTAL PLANE) FRONT VIEW (CORONAL PLANE)
(G) = GLABELLA (P) = PUPIL (T) = TRAGION (I) = INFRAORBITALE
0 — 10 - INCHES

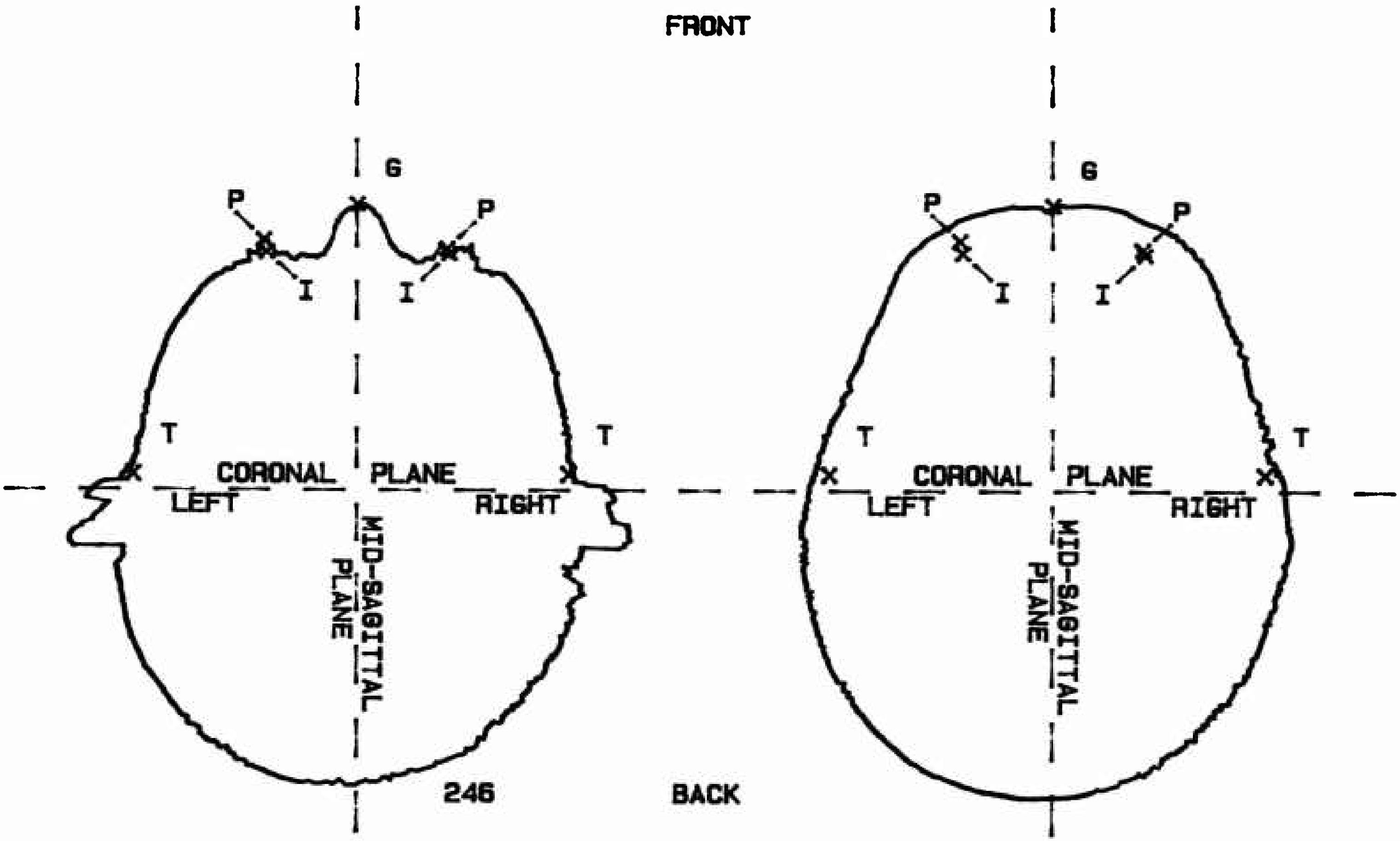

CROSS SECTION AT PUPIL

CROSS SECTION AT GLABELLA

(G) - GLABELLA (P) - PUPIL (T) - TRAGION (I) - INFRAORBITALE

0 —— 10 - INCHES

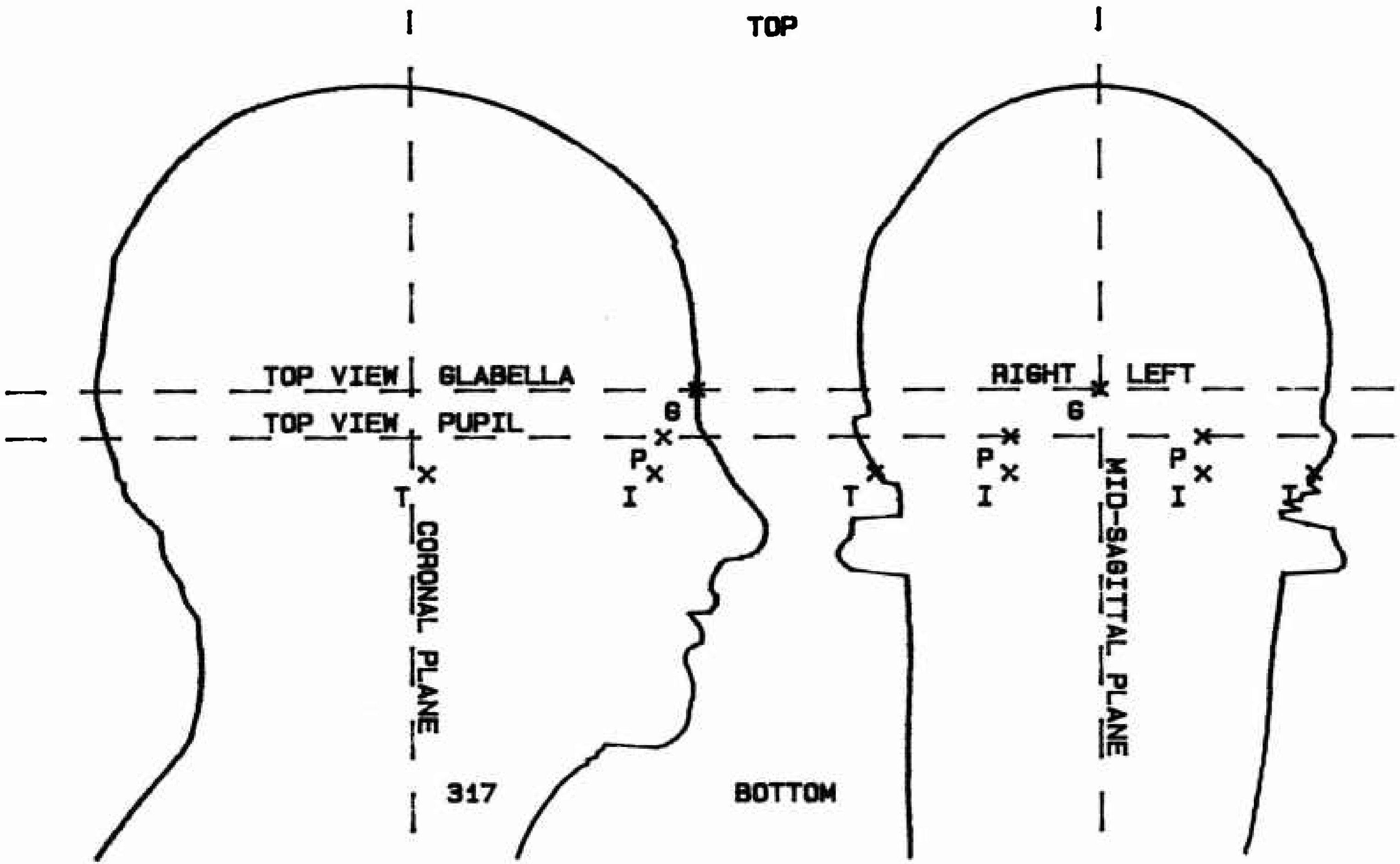

RIGHT SIDE VIEW (MID-SAGITTAL PLANE)   FRONT VIEW (CORONAL PLANE)
(G) = GLABELLA (P) = PUPIL (T) = TRAGION (I) = INFRAORBITALE
0 — 10 - INCHES

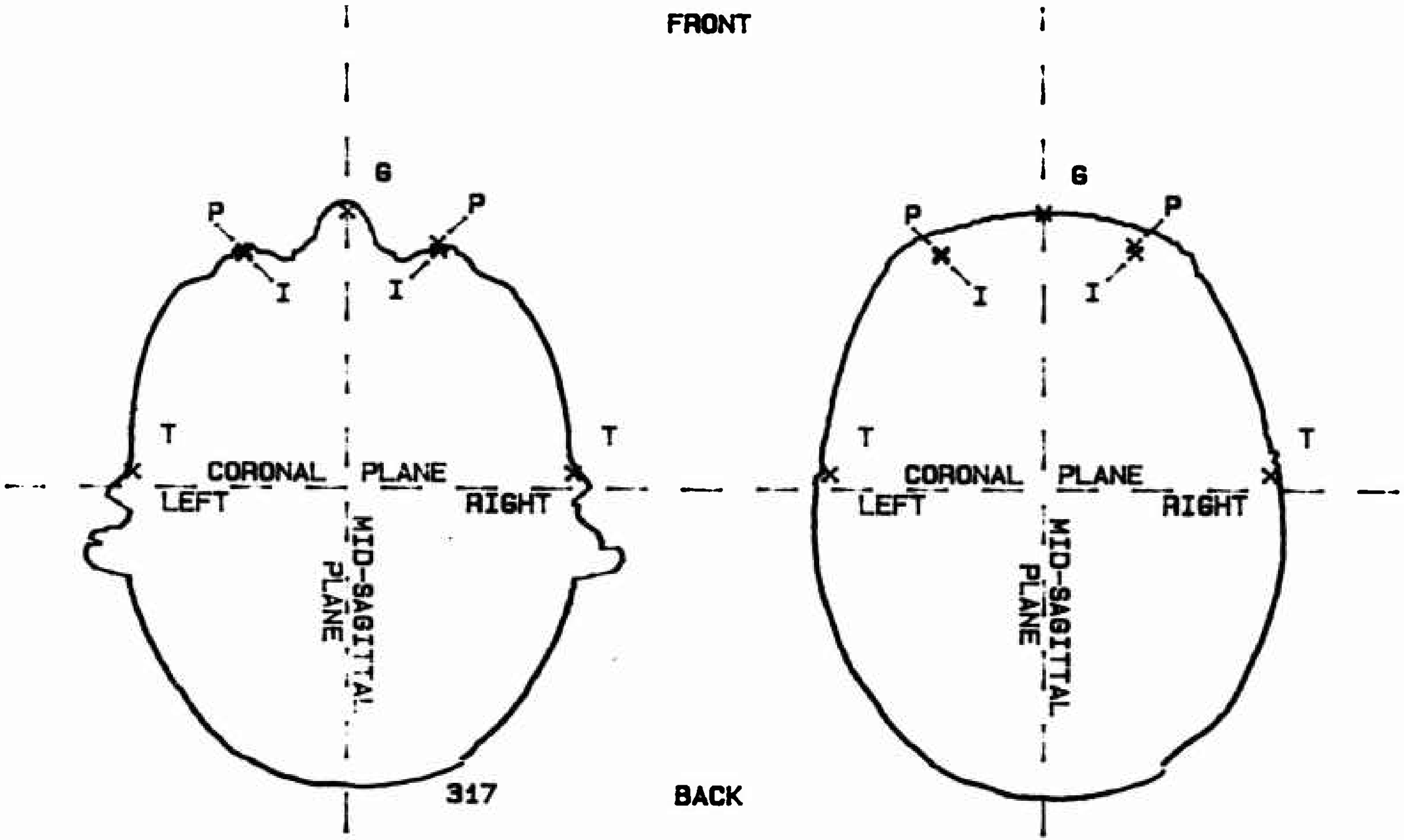

CROSS SECTION AT PUPIL CROSS SECTION AT GLABELLA

(G) = GLABELLA (P) = PUPIL (T) = TRAGION (I) = INFRAORBITALE

0 — 10 - INCHES

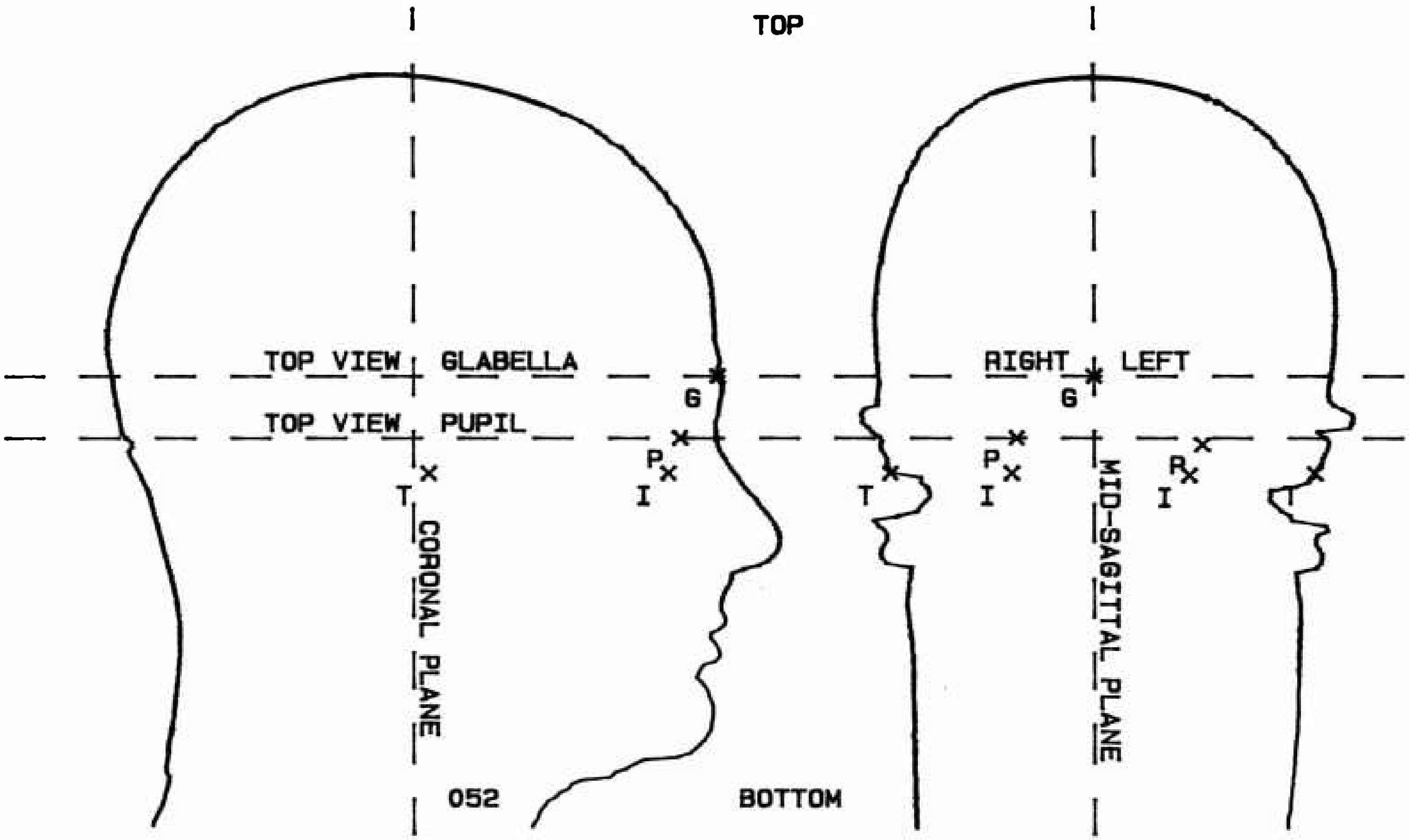

RIGHT SIDE VIEW (MID-SAGITTAL PLANE) FRONT VIEW (CORONAL PLANE)
(G) = GLABELLA (P) = PUPIL (T) = TRAGION (I) = INFRAORBITALE
0 — 10 - INCHES

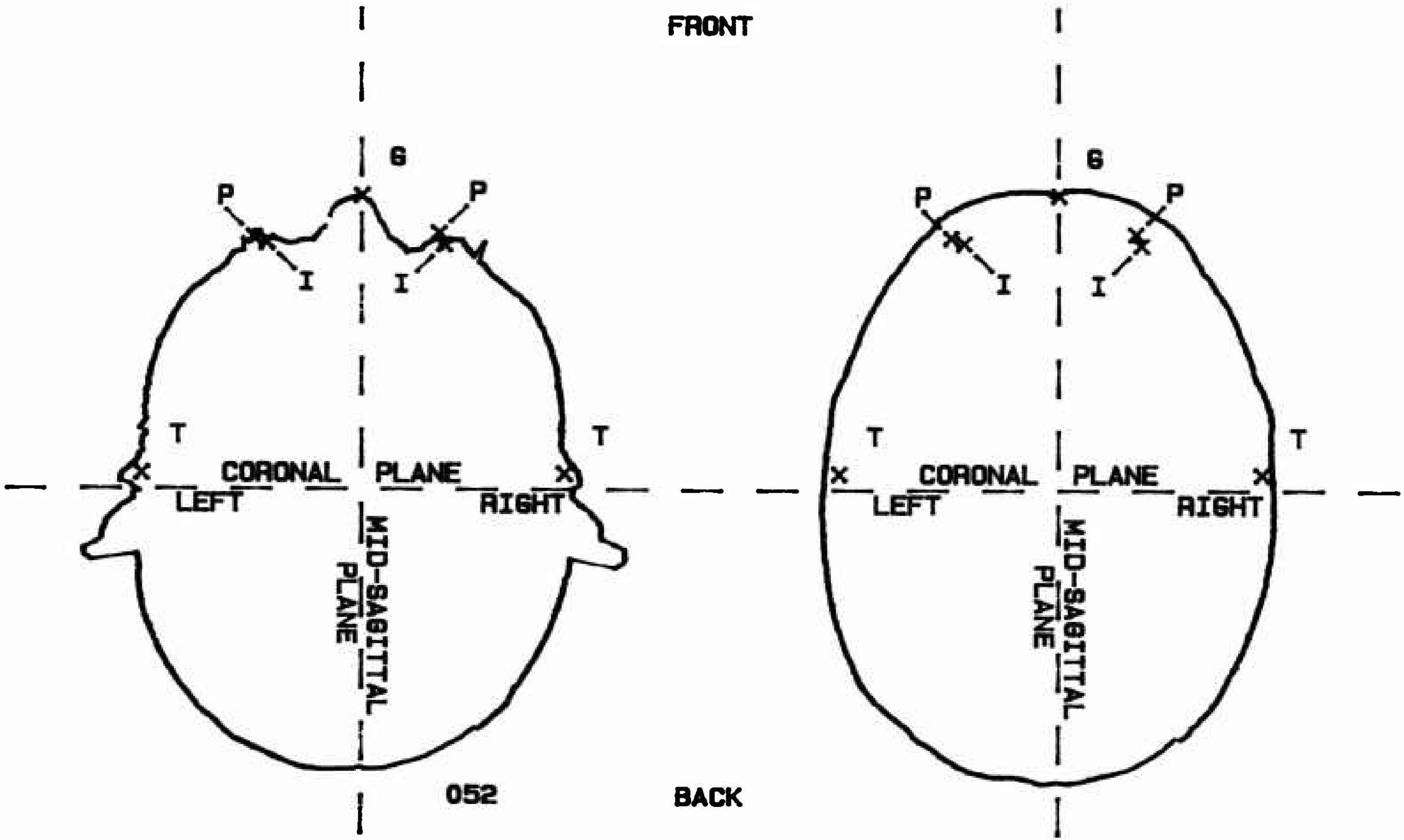

CROSS SECTION AT PUPIL
CROSS SECTION AT GLABELLA

(G) = GLABELLA (P) = PUPIL (T) = TRAGION (I) = INFRAORBITALE

0 — 10 - INCHES

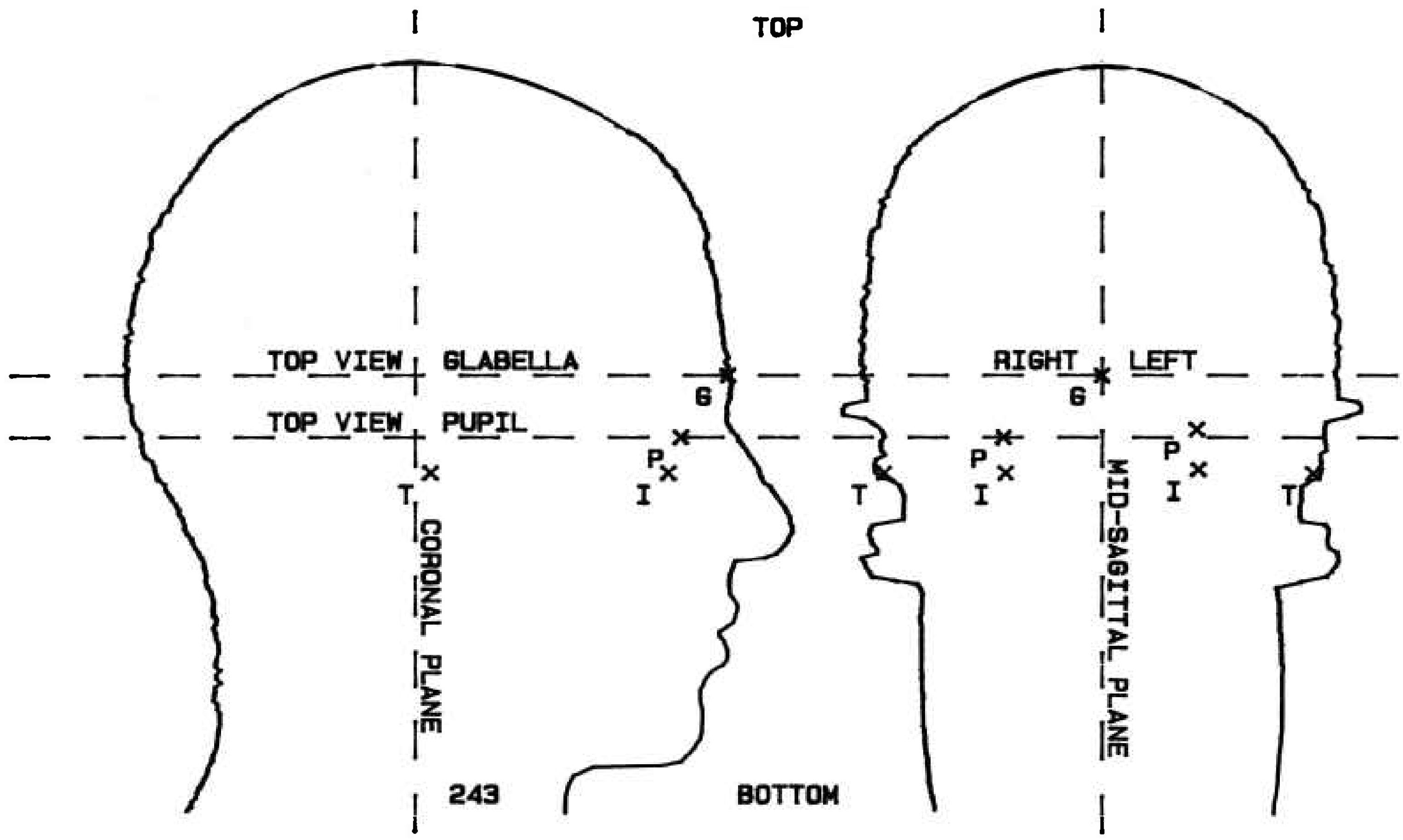

RIGHT SIDE VIEW (MID-SAGITTAL PLANE) FRONT VIEW (CORONAL PLANE)
(G) = GLABELLA (P) = PUPIL (T) = TRAGION (I) = INFRAORBITALE

0 — 10 - INCHES

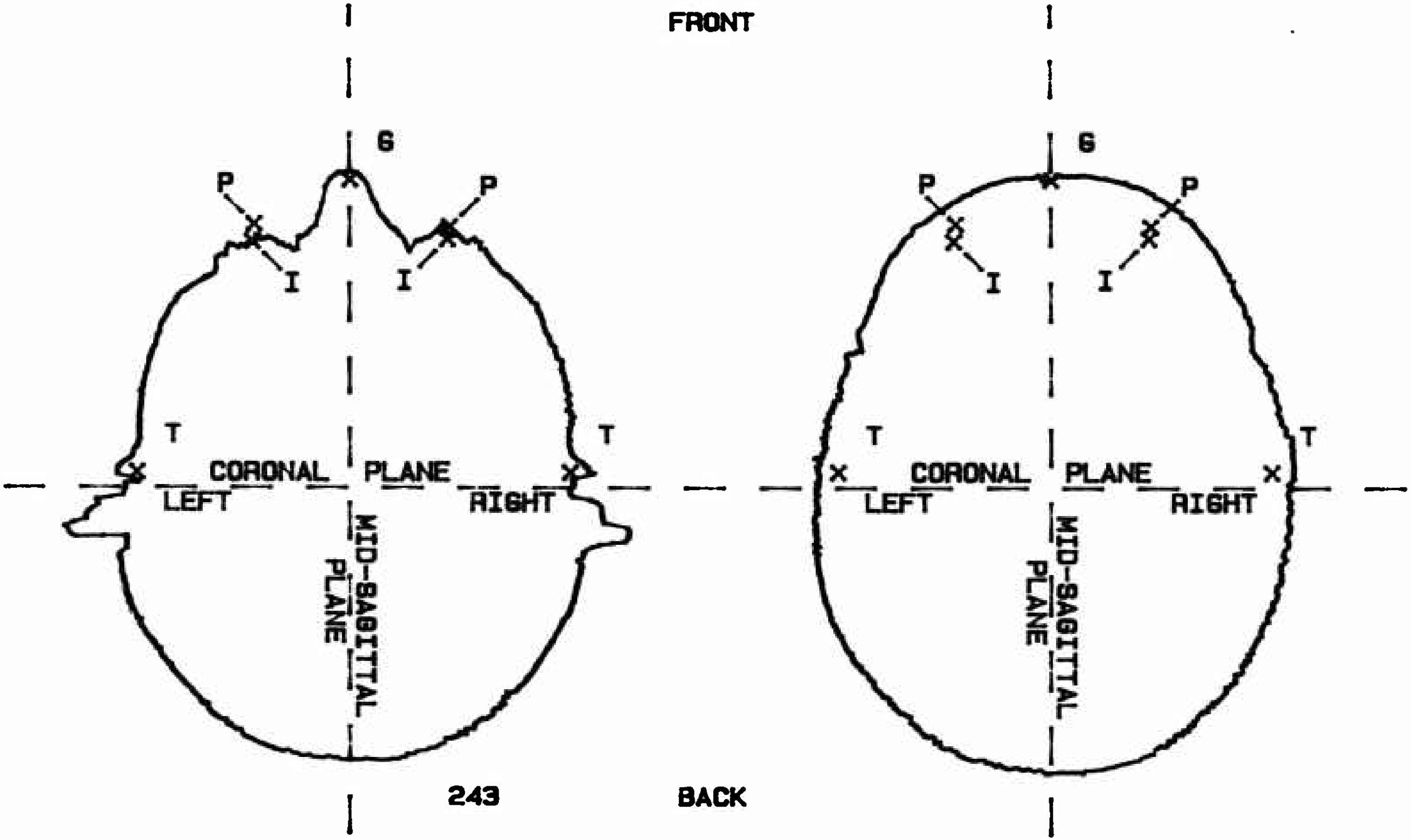

CROSS SECTION AT PUPIL

CROSS SECTION AT GLABELLA

(G) = GLABELLA (P) = PUPIL (T) = TRAGION (I) = INFRAORBITALE

0 — 10 - INCHES

☆U.S. Government Printing Office: 1993 — 750-061/60265